https://doi.org/10.5194/wes-2026-24
Preprint. Discussion started: 10 February 2026

eawe european academy of wind energy
Open Access WIND ENERGY SCIENCE DISCUSSIONS

Evaluating effects of the terrain on modelled winds in multiple atmospheric model datasets

Maksims Pogumirskis[1, 2], Tija Sīle[1], Lasse Svenningsen[2], and Andrea N. Hahmann[3]

[1]Institute of Numerical Modelling, Faculty of Science and Technology, University of Latvia, Riga, Latvia
[2]EMD International A/S, Aalborg, Denmark
[3]Wind Energy Department, Technical University of Denmark, Roskilde, Denmark

Correspondence: Maksims Pogumirskis (maksims.pogumirskis@lu.lv)

Abstract. Numerical atmospheric models are widely used as a meteorological data source when planning the locations of new wind farms. However, before relying on model output for decision-making, it must be verified against observations. Due to commercial restrictions on the availability of observation data, previous studies on atmospheric model validation for wind energy applications are often limited to a single model or a small geographical region. This work performs a large-scale validation of modelled winds at wind turbine heights from seven model datasets against data from more than 500 observation campaigns across Europe. Principal component analysis is used to identify spatial, diurnal, and seasonal patterns of wind speed and direction biases. The results of the analysis show that all seven models exhibit similar spatial and temporal patterns of wind speed bias. Models generally show a more positive wind-speed bias in the Central European Plain and a more negative bias in mountainous regions, namely Southern Europe and the Scandinavian Mountains. Moreover, the temporal patterns of biases also differ between these regions, and wind direction bias shows the same temporal and spatial patterns as the wind speed bias. We show that these wind speed and direction biases can be explained by differences in terrain height between the models and the real world. The magnitude of the wind speed bias ranges from 0.1 to 0.9 ms^{-1} per 100 m of elevation difference, depending on the season and time of day. Two WRF model simulations with different terrain source data are performed, and the modelled winds are compared to provide more robust support for the hypothesis. The results of this work suggest that improving terrain representation in the models can help improve their performance.

1 Introduction

Global warming, which is primarily driven by anthropogenic greenhouse gases, is a major threat to both humans and ecosystems. In 2016, 196 countries signed the Paris agreement with goals of limiting global warming to 2 °C, preferably 1.5 °C, compared to pre-industrial levels (United Nations Climate Change (UNFCCC)). In pursuit of implementing the agreement, the European Union has set the goal of reaching 45 % share of renewable energy by 2030. To reach the goal, wind turbines with a total capacity of at least 37 GW have to be installed each year (European Commission, 2023).

Wind farms are usually installed in locations with high wind resource to maximise their profits. When planning the locations of new wind farms, it is necessary to acquire precise information about the wind climate at their potential locations. Wind

https://doi.org/10.5194/wes-2026-24
Preprint. Discussion started: 10 February 2026

eawe european academy of wind energy
Open Access WIND ENERGY SCIENCE DISCUSSIONS

power density is proportional to the cube of wind speed. Therefore, a small error in the wind speed estimates of 5 % can cause an error of up to 15 % when estimating wind power production.

Direct measurements provide the most precise information about wind conditions. While the World Meteorological Organization (WMO) observation station network is broad and uniformly covers most of the land, it provides only surface wind observations at 10 m height, which are less useful for estimating the wind at turbine height. Measurement availability at heights that are relevant for wind energy (between 50 and 300 m) is limited. Measurements at such heights require the use of expensive equipment such as tall wind masts or remote sensing devices such as lidars or sodars. Moreover, to acquire a meaningful amount of data, the measurement campaign has to be performed for at least a year, which requires regular equipment maintenance. During the measurement campaign, wind data is acquired only for a particular location. Additionally, wind measurements are highly sensitive to the terrain and other obstacles in the close proximity. Therefore, a separate measurement campaign has to be conducted at each potential wind farm location.

Numerical modelling is an alternative way to acquire information about the wind climate of a site, and it has several advantages over direct measurements. It allows to produce spatially and temporally continuous wind data. Moreover, running numerical models is much faster and cheaper than performing measurements. However, results of numerical models should not be relied on without verifying that they match observations, and their limitations are well understood.

Previous studies that have verified atmospheric models against observations for wind energy applications are usually limited to a single model, e.g. CERRA (Jourdier et al., 2023; Rouholahnejad et al., 2024), NEWA (Dörenkämper et al., 2020; Meyer and Gottschall, 2022), NORA3 (Solbrekke et al., 2021), or multiple models in a limited geographical region, e.g., France (Jourdier, 2020), Sweden (Kuru, 2023; Zhi, 2023), North Sea (Cheynet et al., 2022; Spangehl et al., 2023; Kalverla et al., 2020). It has been identified that atmosphere models have systematic issues in representing the observed wind climate. Synoptic scale models usually have horizontal grid spacings of several tens of kilometres, cover the entire globe and are designed to capture large-scale synoptic features such as anticyclones, cyclones and fronts. Studies have shown that due to their coarse resolution, synoptic scale models generally perform worse in complex terrain (Das and Baidya Roy, 2024) or near complex coastlines (Gualtieri, 2021). To improve modelled winds in regions with complex land properties, mesoscale modelled datasets are created by dynamically downscaling synoptic scale model output. Mesoscale models usually have horizontal grid spacings of a few kilometres, cover only a limited area, and can capture winds on finer scales. Studies have shown that mesoscale models outperform synoptic scale models, especially when modelling extreme winds (Solbrekke et al., 2021) or winds in complex terrain (Dörenkämper et al., 2020).

In this work, we perform a large-scale validation of seven atmospheric model datasets for wind energy applications. Winds at heights relevant for wind energy from three global reanalyses and four mesoscale datasets are validated against observations from 508 observation campaigns covering the entire Europe. The aim of the analysis is to identify key systematic differences between modelled and observed winds and physically explain their potential causes. For this purpose, model wind speed biases are analysed in context with wind direction biases. Principal component analysis is used to identify the principal diurnal, seasonal, and spatial patterns of wind speed and direction biases. We explain these wind biases by the differences in how the terrain is represented between models and the real-world.

https://doi.org/10.5194/wes-2026-24
Preprint. Discussion started: 10 February 2026

eawe european academy of wind energy
Open Access WIND ENERGY SCIENCE DISCUSSIONS

Previous studies have identified that models underestimate wind speeds in complex orography (Dörenkämper et al., 2020; Das and Baidya Roy, 2024; Winstral et al., 2016; Hu et al., 2023; Laurila et al., 2021). As complex orography generally coincides with higher elevation above sea level, wind speed bias generally shows a negative correlation with elevation. However, the exact physical causes of the bias are still unclear. The results of this work show that the difference between model and real-world elevation provides significantly stronger statistical explanatory power for the model bias than the real-world elevation alone. It is further shown that the elevation difference between the model and the real-world has an effect not only on the average wind speed bias, but also on the wind direction bias and their diurnal and seasonal cycles. Two WRF model simulations with different terrain source data are performed, and the modelled winds are compared to provide more robust support for the hypothesis.

Further in the work it is discussed which physical processes are potentially affected by the difference in the terrain elevation between models and the real-world. However, regardless of the exact physical cause of the bias, the correlation between model bias and the elevation difference between the model and the real-world suggests that improving terrain representation in atmospheric models has the potential to improve their performance in modelling winds.

2 Data and methods

2.1 Data

2.1.1 Model datasets

In this work, the winds from seven different model datasets were validated against the observations. This includes three global reanalyses: ERA5, MERRA2 and JRA-3Q and four mesoscale model datasets derived from the ERA5 reanalysis by performing dynamical downscaling: NORA3, CERRA, NEWA, and EMD-EUR+. General information about model datasets is compiled in Table 1.

The ERA5 (Hersbach et al., 2020) is a global reanalysis developed by the European Centre for Medium-range Weather Forecasts (ECMWF). ERA5 is based on the Integrated Forecasting System (IFS) modelling system. It provides hourly data of the estimated state of the atmosphere with a resolution of 0.25°or ≈28 km. Such resolution is one of the finest for global reanalyses. Near surface wind data from ERA5 are available either on height levels or native model levels. Data on height levels are limited to only 10 m and 100 m, which is fewer levels than in the case with mesoscale models. However, ERA5 data on native model levels are labelled for expert users and are used less commonly for practical applications. Therefore, for simplicity, in this work only 10 m and 100 m winds from the ERA5 were used.

There is a known systematic issue with winds at lower model levels in the ERA5. Jourdier (2020) has shown that 10 m, 100 m and lower model level winds in ERA5 experience a sudden artificial drop in value at the start of the assimilation window at 9:00 UTC. Wind speeds slowly recover by the end of the assimilation window at 21:00 UTC. Downscaled mesoscale products can potentially inherit the issue, as they use initial and boundary conditions from ERA5. While this issue is not the main focus of the study, it was briefly examined whether or not it is inherited in downscaled mesoscale models.

https://doi.org/10.5194/wes-2026-24
Preprint. Discussion started: 10 February 2026

eawe european academy of wind energy
Open Access WIND ENERGY SCIENCE DISCUSSIONS

The NEWA (Hahmann et al., 2020) is a mesoscale atmospheric dataset based on the open-source Weather Research and Forecasting (WRF) modelling system. It has been developed as an ERANET+ project. The model is run on 27–9–3 km nested domains, where the outer low-resolution domain provides boundary conditions for inner domains. The outer 27 km domain covers a region beyond Europe. A total of ten different overlapping smaller 9–3 km nested domains are used to cover the region of interest. The final dataset with 3 km grid spacing is acquired by spatially stitching together results from all ten 3 km domains and extends over the European Union, the United Kingdom, Norway, Switzerland, Balkans, Turkey, and nearby offshore areas. NEWA provides output every 30 minutes. However, to match other model datasets, only data at full hours were used.

The WRF model used in NEWA is reinitialised every 7 days and run for 8 days. The first 24 hours are used as a spin-up time, and therefore discarded. Meanwhile, the remaining 7 days contribute to the dataset. Spectral nudging to ERA5 reanalysis is performed in the outer domain only above the planetary boundary layer. The NEWA simulations use boundary conditions and nudging data derived from 6-hourly ERA5 data.

The EMD-WRF EUROPE+ (or EMD-EUR+ for short) (Svenningsen et al., 2020) mesoscale dataset is developed by EMD International A/S. It is based on the WRF modelling system and run on a single large 3 km domain without nesting that covers the entire Europe. The model is reinitialised every 7 days and uses a spin-up time of 24 hours. Spectral nudging to the ERA5 reanalysis is performed above the planetary boundary layer. The EMD-EUR+ simulations use boundary conditions and nudging data derived from hourly ERA5 data.

The CERRA (Ridal et al., 2024) is a mesoscale reanalysis developed by ECMWF. It is based on the HARMONIE-ALADIN modelling system. It has a coarser grid spacing (5.5 km) than the other mesoscale models used. The CERRA dataset provides atmospheric analysis using 3D-VAR data assimilation every 3 hours. Additionally, after each data assimilation, a 6-hour forecast with hourly output is provided. The forecast is extended to 30 hours twice a day: at 0:00 and 12:00 UTC. Documentation of the dataset leaves the choice open for the user on which data to use, when constructing hourly series (Jourdier et al., 2023). In this work, hourly series series were constructed using only forecasts with 1, 2, and 3 hour lead-times.

The NORA3 (Haakenstad et al., 2021) is a mesoscale model developed by the Norwegian Meteorological Institute. It is based on the HARMONIE-ALADIN modelling system and has a spatial grid spacing of 3 km. While other mesoscale datasets used in this work cover the entire Europe, NORA3 covers only the northern part of it. NORA3 is run as a hindcast, which is initialised every 6 hours using data from ERA5 reanalysis. The hindcast is run for 9 hours, using the first 3 hours as a spin-up time. NORA3 assimilates only temperature and air humidity observations. The upper-air temperature, humidity, and wind components are interpolated from the host reanalysis ERA5.

The MERRA2 (Gelaro et al., 2017) is a global reanalysis developed by the National Aeronautics and Space Administration (NASA). MERRA2 is based on Goddard Earth Observing System (GEOS) modelling system. It provides hourly atmospheric data with $0.5^\circ \times 0.625^\circ$ resolution. Wind speeds are provided at 10 m and 50 m heights.

The JRA-3Q (Kosaka et al., 2024) is a global reanalysis developed by the Japanese Meteorological Agency (JMA) and is based on the JMA global Numerical Weather Prediction (NWP) system. The spatial resolution of the JRA-3Q is 0.375°. JRA-3Q provides the analysis of the atmosphere every 6 hours. Additionally, forecast data with 3 and 6 hour lead-times are provided. For consistency purposes, in this work, 3-hourly time series were constructed using only forecast data. The only

https://doi.org/10.5194/wes-2026-24
Preprint. Discussion started: 10 February 2026

eawe european academy of wind energy
Open Access WIND ENERGY SCIENCE DISCUSSIONS

Table 1. Summary of model datasets and their characteristics.

Model	Horizontal grid spacing	Height levels used	Temporal resolution	Vertical levels	Region	Modelling system
ERA5	0.25°	10 m, 100 m	1 h	137	Global	IFS
MERRA2	0.5° × 0.625°	10 m, 50 m	1 h	72	Global	GEOS
JRA-3Q	0.375°	8 native model levels	3 h	100	Global	JMA global NWS
NORA3	3 km	50 m, 100 m, 250 m	1 h	65	Northern Europe	Harmonie-Arome
NEWA	3 km	50 m, 75 m, 100 m, 150 m, 200 m	30 min (1 h used)	61	Europe	WRF
CERRA	5.5 km	50 m, 75 m, 100 m, 150 m, 200 m	1 h	106	Europe	Harmonie-Arome
EMD-EUR+	3 km	50 m, 75 m, 100 m, 150 m, 200 m	1 h	50	Europe	WRF

height level at which JRA-3Q outputs winds is 10 m. However, JRA-3Q reanalysis provides data on 8 native model levels in the lowest approximately 300 m of the atmosphere. Therefore, wind data on native model levels were used. As the model is run on hybrid vertical levels, exact heights AGL of these levels differ between model time-steps and geographical locations.

Although JRA-3Q was released in 2018, studies that have assessed its performance for wind energy applications are limited to China (Mi and Liu, 2024). This is likely due to the fact that it is only licenced for non-commercial use. However, its predecessor JRA55 has been widely validated for wind energy applications, e.g. Miao et al. (2020); Das and Baidya Roy (2024). While JRA55 has generally shown poorer performance than ERA5 in modelling winds at turbine heights (Ramon et al., 2019), JRA55 uses significantly different approaches when modelling winds than other global reanalyses. Firstly, based on the results of Carvalho (2019); Belmonte Rivas and Stoffelen (2019), JRA55 is the only global reanalysis that did not show systematic clockwise wind direction bias over the oceans in the Northern Hemisphere, which is a long-known issue in atmospheric models (Hollingsworth, 1994). Secondly, as reported by Torralba et al. (2017), JRA55 is the only global reanalysis that assimilates surface wind speed observations over the land, which allows JRA55 to show good performance in modelling inter-annual wind speed variation and trends on decadal timescales.

2.1.2 Observation dataset

In this work, we verify the model output against the EMD's internal database of wind mast data. The database contains time-series of wind observations from wind masts and remote sensing devices since the 1980's at different heights up to 300 m above ground level (AGL). The database contains data from over 1000 observation locations around the globe.

https://doi.org/10.5194/wes-2026-24
Preprint. Discussion started: 10 February 2026

eawe european academy of wind energy
Open Access WIND ENERGY SCIENCE DISCUSSIONS

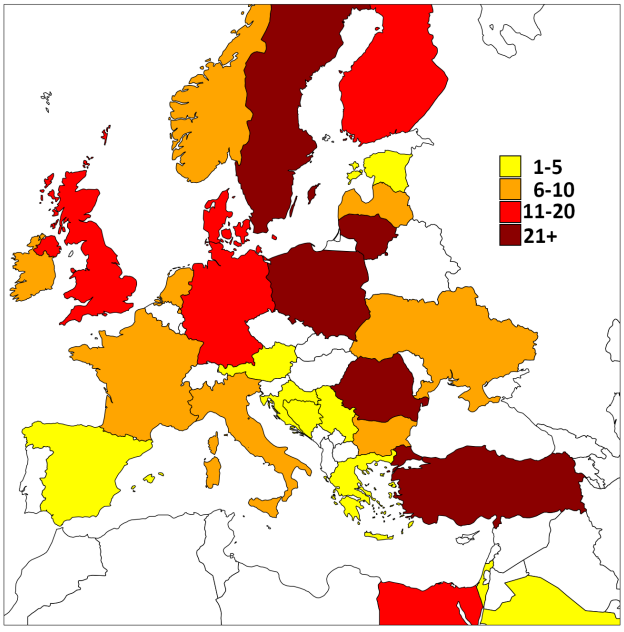

Figure 1. Region of interest and approximate number of observation locations included in the study by country. Countries are categorically coloured based on the number of observation locations included in the study. No observation data were used from countries coloured in white (including microstates).

This work focusses on Europe. Due to data confidentiality, exact locations of observation locations cannot be disclosed. The region of interest and the approximate number of observation locations per country are shown in Figure 1. It should be noted that offshore measurement campaigns were also included in the work, which are counted towards country in which exclusive economic zone it is located. In further figures, Kriging is used to present spatial patterns of biases, while hiding the exact locations of observations. As this work focusses on analysing diurnal and seasonal patterns of model biases, data only form observation campaigns that lasted longer than one year were used in the work. Observations at heights of 50 m or higher AGL were included in the analysis. In total data from 508 observation locations were included in the work; 340 of these locations observations were conducted at heights between 50 (including) and 100 m (excluding), 134 locations at heights between 100 and 150 m and 34 locations at 150 m or higher. 289 observation campaigns lasted between 1 and 2 years, 118 campaigns lasted between 2 and 3 years, 49 campaigns lasted between 3 and 4 years, and 52 campaigns lasted 4 years and more. Most of the campaigns cover some subperiod between 2000 and 2024. Due to the different spatial and temporal coverage of the model datasets, not all observation campaigns were verified against all model datasets.

Basic quality control of the observation data was performed. Obviously erroneous values were excluded: wind direction outside the range $[0°, 360°)$ and wind speed outside the range $[0, 100]$ m s^{-1}. Periods with more than three consecutive 0 m s^{-1} wind speed measurements were excluded, as those are likely to be improperly labelled missing observations.

https://doi.org/10.5194/wes-2026-24
Preprint. Discussion started: 10 February 2026

The frequency of observations is either 1 hour or 10 minutes, depending on the particular observation campaign. On the other hand, model output is provided hourly or every three hours. For comparison purposes, observed values were averaged to the hourly resolution.

2.2 Methods

2.2.1 Comparing models with observations

The bias metric was used to quantify the differences between the models and the observations. Bias is defined as the average difference between modelled and observed values. For wind energy applications, accurate predictions of the wind speed are generally assumed to be more relevant than the wind direction. However, in this work, a holistic analysis is performed and wind speed biases are considered in context with wind direction biases to seek their physical explanation.

The positive wind speed bias indicates that the model overestimates the wind speed, while the negative wind speed bias indicates that the model underestimates the wind speed. As the wind direction is a circular variable, the bias metric cannot be applied directly. To address this issue, 360°was added to the observed wind direction when necessary to ensure that the difference between the modelled and observed values is between -180°and 180°. Positive wind direction bias indicates that modelled winds are more clockwise than the observed ones, while negative wind direction bias indicates that modelled winds are more anti-clockwise than the observed ones.

We analyse spatial, diurnal, and seasonal patterns of wind speed and direction biases. For this purpose, each observation location was described by a 24×12 variables – mean differences between modelled and observed winds aggregated by the hour of day and month of the year. In the case of the JRA-3Q reanalysis, 8×12 variables were used, since it provides an output every 3 hours. Principal component analysis was applied to seek temporal and spatial patterns of model biases (described later).

When comparing the model with the observations, the model data from the closest horizontal grid cell to the observation campaign location were used without considering any land properties. Vertically, data were interpolated from two adjacent model levels above ground level to the observation height above ground level. Wind speed was interpolated using the power law, i.e., assuming that the logarithm of wind speed is a linear function of the logarithm of the height. The wind direction was interpolated considering it as a unit vector and linearly interpolating its components.

When interpolating wind speeds between different heights, it should be considered that models use different methodologies when calculating 10 m winds and winds at higher levels of the atmosphere. The 10 m wind speed is usually a diagnostic variable and is not modelled directly. For example, in ECMWF forecasts 10 m winds are interpolated from the lowest model level (Owens and Hewson, 2018). The roughness length of the short grass (0.03 m) which matches recommended WMO observation conditions is used instead of the actual roughness length of the model grid-cell. Therefore, the use of modelled 10 m winds should be generally avoided, when interpolating winds to higher levels.

To interpolate the wind speed to any given height, wind speed values at least at two different heights are needed. All mesoscale models provide wind data at multiple heights, covering the entire range of wind mast observation heights. Therefore, using 10 m wind speeds can be avoided. However, ERA5 provides wind speeds only on 10 m and 100 m heights, and MERRA2

https://doi.org/10.5194/wes-2026-24
Preprint. Discussion started: 10 February 2026

eawe european academy of wind energy
Open Access WIND ENERGY SCIENCE DISCUSSIONS

provides wind speeds on 10 m and 50 m heights, which makes use of 10 m winds unavoidable. This should be considered when interpreting the results from ERA5 or MERRA2.

2.2.2 Principal component analysis

Due to high maintenance costs, observation campaigns are usually kept as short as possible, usually being just over a year and rarely exceeding three years. While such duration is usually sufficient for decision-making regarding wind farm installation, it might not be sufficiently long to be able to identify systematic biases of models, when comparing model output to observations from an individual mast. In climate sciences, a 30 year period is usually used to define systematic weather patterns, i.e., climate normals.

The motivation of the analysis is based on the assumption that the model output differs from the real-world conditions because some physical phenomena in the model are improperly represented. Each improperly represented phenomenon contributes to the total model bias by amplifying or cancelling the effects of other phenomena. To improve future atmospheric models, it is important to decompose the total model bias into contributions from each improperly represented physical phenomenon and individually fix them.

Principal component analysis (PCA) is a statistical technique that is commonly used to identify the main patterns in large and noisy multidimensional datasets (Jolliffe, 2002). The method considers correlations between original variables and derives new variables (principal components or PC for short) that are linear combinations of the original variables. New variables are created in such a way that the first principal component (PC1) explains the maximum possible variance of the data and each subsequent principal component (i.e., PC2, PC3, ...) is uncorrelated with all previous PCs while explaining the maximum possible remaining variance of the data. Therefore, only a few of these new variables are needed to describe the main features of the dataset. The values of the principal components describe how prominent each feature is for a particular data point. The principal components can be interpreted as unit vectors that describe the axes along which the data points differ from the mean values of the dataset. The linear coefficients of each principal component are known as "loadings", which can be interpreted as the vector components. Previous work has successfully applied PCA to identify seasonal patterns of meteorological variables such as wind direction (Pogumirskis et al., 2021) or temperature and precipitation (Bethere et al., 2017).

PCA is suitable for tackling the data issues described above. Firstly, it allowed to look at biases at a single observation location in context with other locations, therefore allowing to identify biases even if only one year of observational data was available at the particular location. Secondly, PCA allowed to identify main features of the dataset, which made it easier to decompose the causes of the average bias in the model into simpler components, making it easier to link them with particular geographical locations or physical phenomena. Moreover, decomposition allows to estimate how model output would improve if certain model issues were fixed.

In this work, the PCA was performed separately for each model and for wind speed and wind direction. Bias at a particular location was described by 24×12=288 (8×12=96 in the case of JRA-3Q) parameters – bias values for the particular month or hour of the day. Lets denote the bias table at a location i as X_i. By taking the average value of the tables between all observation locations, we can compute the average bias of the model — $\bar{X}$, which is also a 24×12 table. These bias tables

https://doi.org/10.5194/wes-2026-24
Preprint. Discussion started: 10 February 2026

eawe european academy of wind energy
Open Access WIND ENERGY SCIENCE DISCUSSIONS

at each observation location can be viewed as points in a 288 dimensional space centred at zero. Initially, data are defined in the canonical orthonormal basis where each of 288 unit vectors $\boldsymbol{e_j}$ has 1 at position j and 0 at the other 287 positions. By applying PCA a coordinate transformation is performed, which centres the coordinate axis at the mean bias $\bar{X}$ and rotates the unit vectors $\boldsymbol{e_j}$ so that they match the principal components as described before. After the coordinate transformation, model biases can be expressed in new coordinates where principal components (i.e., PC1, PC2, ...) are the unit vectors, "loadings" are components of these vectors, and $y_{i,j}$ are the coordinates of points in the new coordinate system (known as "values" of principal components), where i denotes the observation location and j denotes the rank of the principal component. The bias table at a particular location i in the new coordinates can be expressed as:

$$X_i = \bar{X} + y_{i,1} \cdot PC1 + y_{i,2} \cdot PC2 + \ldots + y_{i,288} \cdot PC288. \tag{1}$$

Since principal components are ranked by the amount of information they explain, a first few principal components can explain the main model biases. In the further analysis, it was attempted to link the most significant principal components to some physical phenomena that are improperly represented in models.

When performing PCA an important question to consider is whether a normalisation of initial variables is needed. In this work a comparison between biases was performed in absolute values, i.e., in $\mathrm{m\,s^{-1}}$ for the wind speed bias and in degrees for the wind direction bias. Therefore, no normalisation of the initial values was performed.

When presenting results of the PCA, normalisation of values of the principal components and loadings was performed. Initially loadings of a principal component are dimensionless and the sum of their squares add up to 1. The values of the principal components are in $\mathrm{m\,s^{-1}}$ or degrees. However, they cannot be easily interpreted since the magnitude of those values is affected by the number of dimensions. To provide a better physical interpretation, values of each principal component were divided by the standard deviation of the particular principal component between observation locations, making them dimensionless. On the other hand, loadings were multiplied by the standard deviation of the particular principal component between observation locations, setting their dimension to $\mathrm{m\,s^{-1}}$ or degrees.

After normalisation is applied, the value of the principal component describes the prominence of the bias described by that principal component at a particular location. The standard deviation is chosen as an interpretable measure, since in the case of the normal distribution 99.7 % of the data lie within 3 standard deviations of the mean. On the other hand, loadings describe a characteristic magnitude of the bias in the dataset — the magnitude of the bias at a location where the value of a principal component is 1 standard deviation from the mean.

2.2.3 Terrain representation

Previous studies (Dörenkämper et al., 2020; Das and Baidya Roy, 2024; Winstral et al., 2016; Hu et al., 2023; Laurila et al., 2021) have identified that the wind speed bias is more negative in complex terrain. However, a negative wind speed bias in complex terrain can be caused by numerous different factors and these causes are still unclear. Possible causes of the bias include model inability to resolve small scale terrain features (Das and Baidya Roy, 2024), errors in estimating orographic drag (Sandu et al., 2017) and errors in estimating orographic speed-up (Jiménez and Dudhia, 2012). This work attempts to provide a

https://doi.org/10.5194/wes-2026-24
Preprint. Discussion started: 10 February 2026

physical explanation of the negative wind speed bias in complex terrain. Our hypothesis is that the wind speed bias in complex terrain is caused by the differences in elevation between the model and the real-world terrain. The terrain in models is spatially aggregated, and it is a smoothed version of the real-world terrain. Therefore, the elevation of the observation location does not always coincide with the elevation of the model grid point. Hence, when comparing models with observations, essentially winds over two different terrains are compared.

Differences in terrain representation between models and the real world can affect modelled winds in numerous different ways. This work focuses on identifying model biases that are caused by the local processes. In other words, model bias at a particular grid-point is present because the elevation of a grid-cell is different from the terrain elevation at the observation location. These effects can be identified by considering the correlation of model bias and elevation difference between the model and the real-world. As the atmosphere is in continuous motion, wind biases can propagate spatially. Therefore, if the model underestimates the winds at a particular location, it would likely underestimate the winds downwind of that location. While this work focusses only on describing local biases caused by terrain differences, it is reasonable to assume that fixing local model biases would improve model performance non-locally.

To test the hypothesis, we analysed how well model bias statistically can be explained by the difference between the model and real-world elevation versus the case where only the real-world elevation is considered. For such purpose we performed stepwise linear regression. In the first case, only the real-world elevation was used to linearly predict values of the principal component of model bias. In the second case, both the model and the real-word elevation were considered as predictors. The F-test was used to evaluate whether the increase in correlation is significant when both the model and the real-world elevation is used to explain the model biases versus the case when only the real-world elevation is used as the explanatory variable. In all cases, the regression coefficients for the real-world and model terrain had approximately the same magnitude and opposite signs, indicating that bias is explained by their difference. In further work, the linear combination of model elevation and real-world elevation, which predicts model biases using the linear regression, is referred to as the "weighted difference between model and real-world elevation".

The native model elevation at the grid cell used for comparison was used as the "model elevation" variable. Elevation data from Copernicus 3 degree-second (90 m) digital elevation model (DEM) closest to the observation location was used as the "real-world elevation" variable.

2.2.4 WRF modelling

The results of the comparison between models and observations suggested that a significant cause of the differences between the modelled and observed winds is the terrain height difference between models and the real-world. To test the hypothesis, we performed two one-year WRF model simulations using different terrain source datasets, but otherwise the same setup. One run used GMTED2010 terrain input data at 30 s (≈900 m) resolution, while the other used 5 min (≈9 km) resolution. GMTED2010 is the default terrain dataset provided with the WRF model installation at different resolutions. The motivation for using these two terrain datasets to test the hypothesis lies in how the terrain is represented at different resolutions.

https://doi.org/10.5194/wes-2026-24
Preprint. Discussion started: 10 February 2026

eawe european academy of wind energy
Open Access WIND ENERGY SCIENCE DISCUSSIONS

In the real-world, terrain height is a continuous variable, i.e., its resolution is infinitely fine. In the Copernicus dataset used in this work, the terrain is aggregated on a 3 degree-second grid (≈90 m resolution). In the WRF model run that uses 30 s terrain input data, the terrain is aggregated on a 3 km grid, since the model grid is coarser than the input data. Meanwhile, in the WRF model run that uses 5 min input data, the terrain is smoothed, since the input terrain resolution is coarser than the model resolution.

When observations are compared with the 3 km model, the flow over the real-world terrain is compared with the flow over the 3 km terrain, which is a smoothed version of the real-world terrain. Similarly, when modelled winds over the 30 s terrain are compared with modelled winds over the 5 min terrain, the flow over a detailed terrain is compared with the flow over a smoothed version of the same terrain. An illustrative example of a topographic profile in the Copernicus dataset as well as both WRF models is shown in Figure 2. It can be seen that in the Copernicus 3 s DEM hills are generally higher and valleys are generally deeper than in WRF model that uses 30 s terrain input. Similarly, in the WRF model that uses 30 s terrain input hills are generally higher and valleys are generally deeper than in the WRF model that uses 5 min terrain input.

Models and observations generally show differences due to numerous factors. On the other hand, the two models used in this work differ only by their terrain. Therefore, their differences are caused solely by differences in terrain representation. The model that uses 30 s terrain is used as an analogy for the flow in the real world, i.e., with fully resolved terrain. On the other hand, the model that uses 5 min terrain is used as an analogy for the flow in a model, i.e., with an aggregated and smoothed terrain. It is hypothesised that these two models show differences similar to the ones that exist between a model and observations. When comparing models with observations, observed winds were subtracted from the modelled winds. The order in which models were subtracted was chosen to represent the same effects as when comparing models and observations. The output of the 30 s terrain model was subtracted from the output of the 5 min terrain model.

Both WRF model runs were performed on a 810×1620 km domain covering Sweden, consisting of 270×540 grid cells. To avoid domain boundary effects of the low resolution boundary conditions, 10 outer grid cells of both domains were excluded from the comparison. Model domains, and differences in their terrain are shown in Figure 3. The average difference between elevations in both models is 0.4 m, the maximum absolute difference is 490.2 m, and the standard deviation of differences is 35.6 m. Both models used otherwise the same WRF model setup described in Table A1. Hourly winds at 100 m height AGL were used for comparison, since they are close to the typical observation height for the EMD mast database. The analysis was performed using PCA in a similar manner as that applied when comparing models with observations: each of the model grid-points was described by 24×12 variables – average differences in mean wind speed or direction between models for the particular hour of the day or month of the year.

Sweden was chosen as the simulated region due to several factors. First, choosing all of Europe as a domain would significantly increase the computational time. Second, Sweden has a diverse terrain — complex terrain in the north and simple terrain in the south. Moreover, large areas of open sea are present. Third, the EMD mast database has a high observation coverage of the Sweden, which allowed to verify these models against observations for future work. Due to the higher availability of observation data, 2011 was chosen as the year for both runs.

https://doi.org/10.5194/wes-2026-24
Preprint. Discussion started: 10 February 2026

eawe european academy of wind energy
Open Access WIND ENERGY SCIENCE DISCUSSIONS

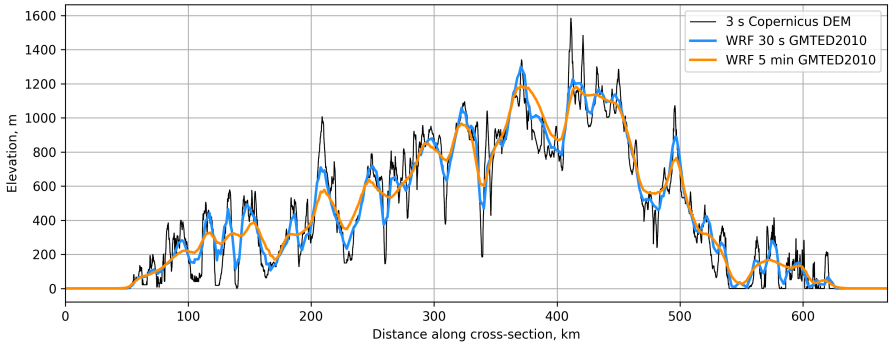

Figure 2. An example of a topographic profile in Copernicus 3 s DEM and both WRF models used in this work. The exact location of the line is shown on the map in Figure 3. Terrain elevation in metres is shown on the y axis and distance along the line in kilometres is shown on the x axis.

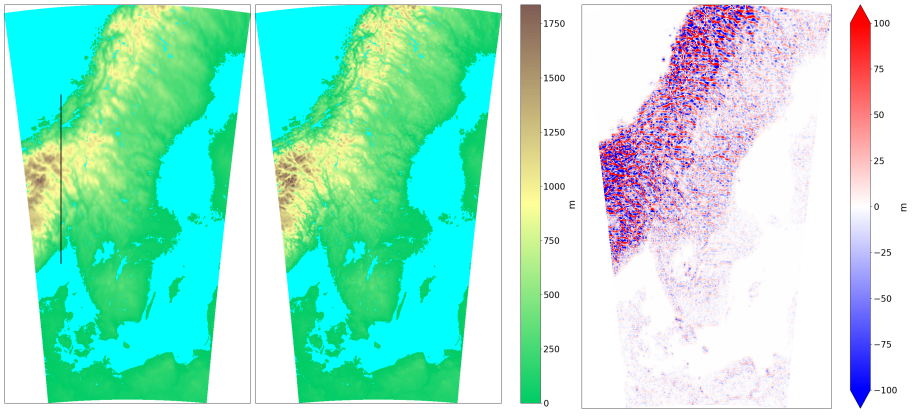

Figure 3. Terrain elevation height in metres and domain extent for both WRF model runs (including the buffer zone). Terrain using 5 min resolution input data is shown on the left, terrain using 30 s resolution input data is shown in the middle and their difference is shown on the right. The line of the topographic profile from Figure 2 is included.

3 Results

3.1 Comparison between models and observations

The results of the principal component analysis suggest that all seven models show similar principal spatial and temporal patterns of the wind speed and direction biases. Temporal patterns of biases in the Central European Plain differ significantly from patterns in mountainous regions — Southern Europe and Scandinavian Mountains. The approximate boundaries of these regions can be seen in Figure 4, which shows the spatial patterns of PC1 values of wind speed bias in the ERA5 reanalysis. Values of PC1 of wind speed bias and values of PC2 of wind direction bias show similar spatial patterns in all seven models.

https://doi.org/10.5194/wes-2026-24
Preprint. Discussion started: 10 February 2026

eawe european academy of wind energy
Open Access WIND ENERGY SCIENCE DISCUSSIONS

However, for brevity, detailed results only for the ERA5 reanalysis are presented in the main part of the paper. For other model datasets, mean biases and loadings of principal components are included in the appendix.

The temporal patterns of the spatially averaged wind speed bias show differences depending on the dataset. In ERA5 (Figure 6, (b)) and MERRA2 the average wind speed bias is more positive during the day and more negative during the night. In NORA3, EMD-EUR+, CERRA, NEWA and JRA-3Q the average wind speed bias is more positive during the winter and more negative during the summer. In NORA3, EMD-EUR+, CERRA, and JRA-3Q the bias is more negative during the day and more positive during sunrise and sunset. In NEWA the wind speed bias is more negative during the day, and the magnitude of the bias is significantly higher than in other models. However, NEWA shows a more positive bias only during sunset and does not show a more positive bias during sunrise.

The principal components describe how the temporal patterns of model biases in different observation locations differ from the temporal pattern of the spatially averaged model bias. For example, the temporal patterns of spatially averaged wind speed bias in ERA5 are shown in (Figure 6, (b)). The loadings of PC1 of the wind speed bias in ERA5 are shown in Figure 5, (a). The temporal patterns of wind speed bias at a particular location can be calculated by combining the spatially averaged temporal pattern of the model wind speed bias with the sum of the values of all principal components at that location, each multiplied by the corresponding principal component. PCA is performed with the goal of linking each principal component to some improperly represented atmospheric phenomena. By setting the values of all principal components except one to zero, it is possible to analyse how model biases in different regions are affected by the improper representation of a particular atmospheric phenomenon. Further in the work PC1 of the wind speed bias (explains 82.5 % of variance in the wind speed bias in the ERA5 reanalysis) and PC1 and PC2 of the wind direction bias (explain 61.1 % and 5.7 % of variance in the wind direction bias in the ERA5 reanalysis, respectively) are analysed. For other models, PC1 of the wind speed bias explains between 61.6 % and 81.3 % of variance, PC1 of the wind direction bias explains between 52.4 % and 68.3 % of variance, and PC2 of the wind direction bias explains between 3.4 % and 6.3 % of variance.

For example, if PC1 of the wind speed bias at a particular location shows a value of negative 1 standard deviation, then the temporal patterns of bias at that location would look more similar to (Figure 6, (a)). Such temporal patterns of wind speed bias are characteristic for mountainous regions, where values of PC1 of the wind speed bias are more negative. In mountainous regions, all models show overall more negative wind speed bias. Wind speed bias is more positive during the day and more negative during the night. However, if PC1 of the wind speed bias at a particular location shows a positive value of 1 standard deviation, then the temporal patterns of bias at that location would look more similar to (Figure 6, (c)). Such temporal patterns of wind speed bias are characteristic to the Central European Plain, where wind speed bias is overall more positive. The bias is more positive during winter than during summer and more negative during the day than during the night.

Temporal patterns of spatially averaged wind direction bias show differences depending on the dataset. In EMD-EUR+, CERRA, ERA5 (Figure 7, (b)) and MERRA2 the wind direction bias is more clockwise during the day and more anti-clockwise during the night. In NORA3 wind direction bias is more clockwise in winter and more anti-clockwise in summer. In NEWA the wind direction bias is more clockwise during the night and more anti-clockwise during the day. In JRA-3Q the wind direction bias is more clockwise closer to sunset.

https://doi.org/10.5194/wes-2026-24
Preprint. Discussion started: 10 February 2026

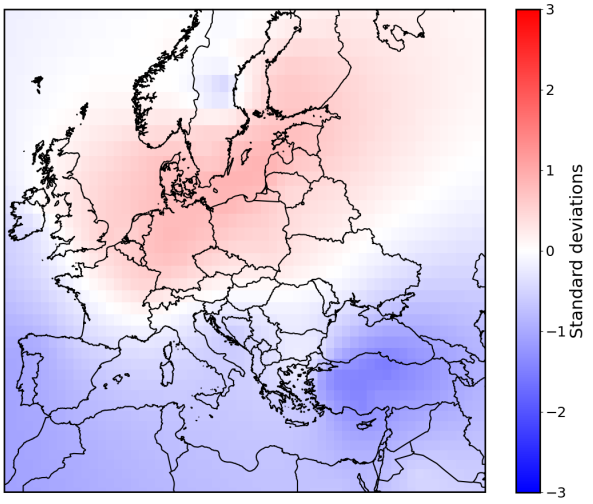

Figure 4. Spatially interpolated values of the PC1 of the wind speed bias in ERA5 reanalysis. Values are normalised by dividing a value of PC1 at each location by the standard deviation of all PC1 values between all observation locations. Units are standard deviations above the average.

Similarly to values of PC1 of the wind speed bias, the values of PC2 of the wind direction bias show differences between parts of Europe – Central European Plain and mountainous regions (Figure 4). The only difference is that the sign of PC2 of the wind direction bias is the opposite to the sign of PC1 of the wind speed bias. That is, values of PC2 of the wind direction bias are negative in the Central European Plain and positive in the mountainous regions. Characteristic patterns of the wind direction patterns for these regions can be acquired by adding loadings of PC2 of the wind direction (Figure 5, (c)) multiplied by the value of PC2 at a particular location to the spatially averaged temporal pattern of the wind direction bias. In the Central European Plain, the values of PC2 of wind direction bias are negative. Therefore, in the Central European Plain, the temporal patterns of the wind direction bias are closer to the ones shown in Figure 8, (a). In the Central European Plain, all models show more clockwise wind direction bias in winter and more anticlockwise wind direction bias in summer. In mountainous regions PC2 of the wind direction bias shows positive values. Therefore, in mountainous regions the characteristic temporal patterns of the wind direction bias are closer to the ones shown in Figure 8, (c). In mountainous regions, the wind direction bias is more clockwise during the day and more anticlockwise during the night. PC2 of the wind direction bias describes only differences in the temporal patterns of the wind direction bias, while PC1 of the wind speed bias describes both differences in temporal patterns and the overall magnitude of the bias (more positive or negative wind speed bias).

The overall magnitude of the wind direction bias (overall clockwise or anticlockwise wind direction bias) is described by the PC1 of the wind direction bias. The loadings of PC1 of the wind direction bias are shown in Figure 5. Positive values of PC1 of the wind direction indicate that wind direction bias at a particular location is overall more clockwise, while negative values indicate that the bias is overall more anticlockwise. The loadings of PC1 of the wind direction bias are different for different months and times of the day. However, when adding (Figure 7, (c)) or subtracting (Figure 7, (a)) 1 standard deviation of values

https://doi.org/10.5194/wes-2026-24
Preprint. Discussion started: 10 February 2026

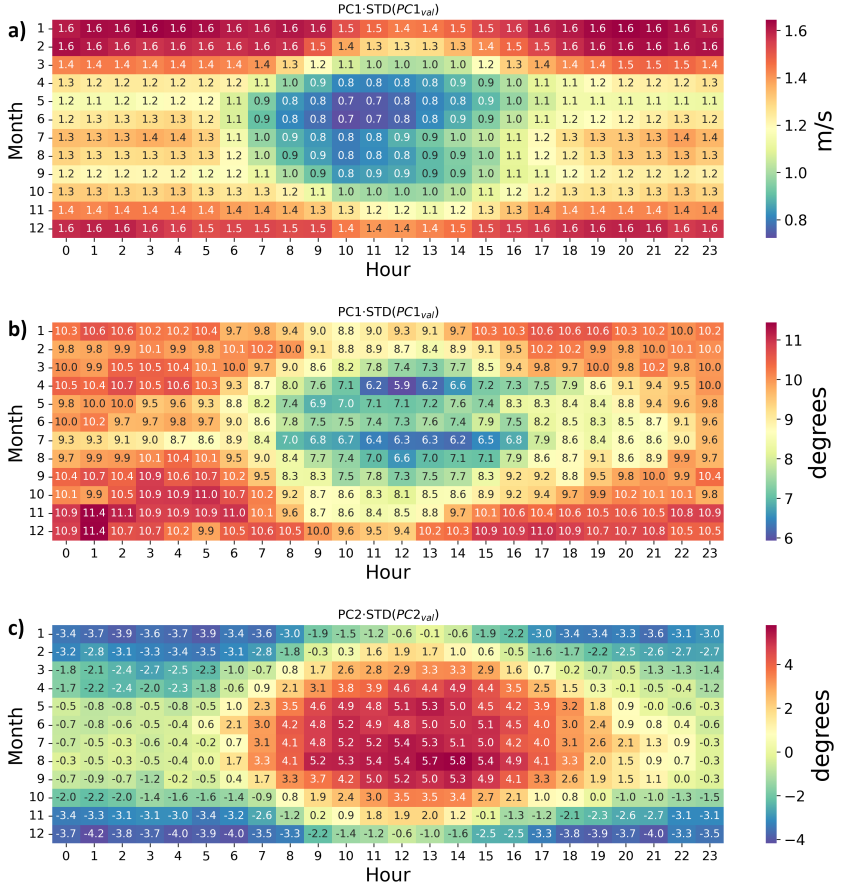

Figure 5. ERA5 reanalysis and observation comparison. Loadings of the PC1 for wind speed bias (a), PC1 of wind direction bias (b) and PC2 of wind direction bias (c). Loadings are normalised by multiplying them by the standard deviation of values of the particular principal component between all observation locations. Units are m s^{-1} for wind speed and degrees for wind direction.

of PC1 of the wind direction bias to the spatially averaged wind direction bias has a much smaller effect on temporal patterns than in the case for PC1 of the wind speed bias and PC2 of the wind direction bias.

All models show similar spatial patterns of values of PC1 of the wind direction bias. However, in contrast to PC1 of the wind speed bias and PC2 of the wind direction bias, values of PC1 of the wind direction bias shows no clear spatial patterns (cannot be shown due to confidentiality reasons). Values of PC1 in the same model can differ significantly even when two observation points are located within the same model grid-cell and in a simple terrain. The standard deviation of the average wind direction bias between observation locations ranges between 8 and 10 degrees depending on the model. The physical interpretation of PC1 of wind direction bias is outside the scope of this paper. However, it can possibly be caused by an improper calibration of the reference wind direction when installing the mast or obstacles in close proximity of the observation campaign that are not resolved in the models.

https://doi.org/10.5194/wes-2026-24
Preprint. Discussion started: 10 February 2026

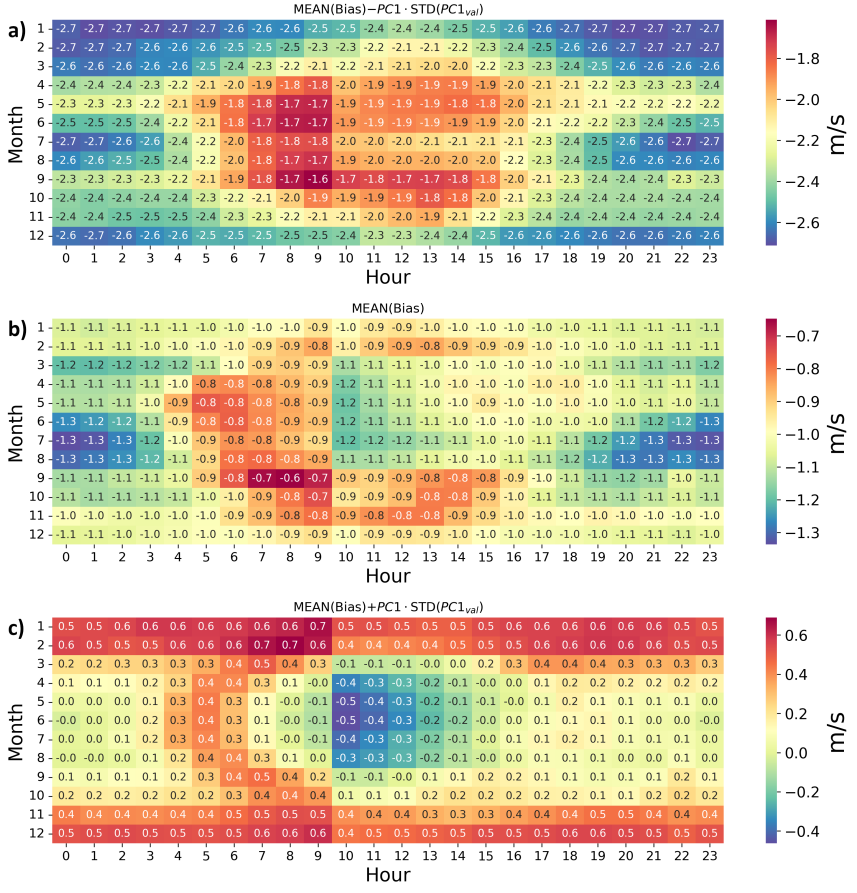

Figure 6. Wind speed biases (in $\mathrm{m\,s^{-1}}$) in ERA5 reanalysis dependent on month (y axis) and time of day (x axis). Spatially averaged bias is shown in (b). (c) shows spatially averaged bias plus 1 standard deviation of values of the PC1 between observation locations. (a) shows spatially averaged bias minus 1 standard deviation of values of the PC1 between observation locations.

To test the hypothesis of whether the biases are caused by differences in the terrain representation between models and real-word, correlations between principal components and terrain variables – real-world elevation, model elevation and their weighted difference were considered. The correlations between elevation variables and the principal components of wind speed and direction biases are summarised in Figure 9. Since the sign of principal components is arbitrary when applying PCA to different model datasets, correlations are multiplied by -1 when necessary to match the sign with the ERA5 as was presented above. For all models and all bias variables, it can be seen that the correlation becomes noticeably stronger when the elevation difference is considered, compared to a case where only the real-world elevation is considered. The results of the F-test show that the increase in correlation is statistically significant in all cases (P<0.05).

The ERA5 reanalysis shows the strongest correlations between elevation difference and bias variables. The correlation is 0.71 for values of PC1 of the wind speed bias and 0.41 and -0.50 for values of PC1 and PC2 of the wind direction bias,

https://doi.org/10.5194/wes-2026-24
Preprint. Discussion started: 10 February 2026

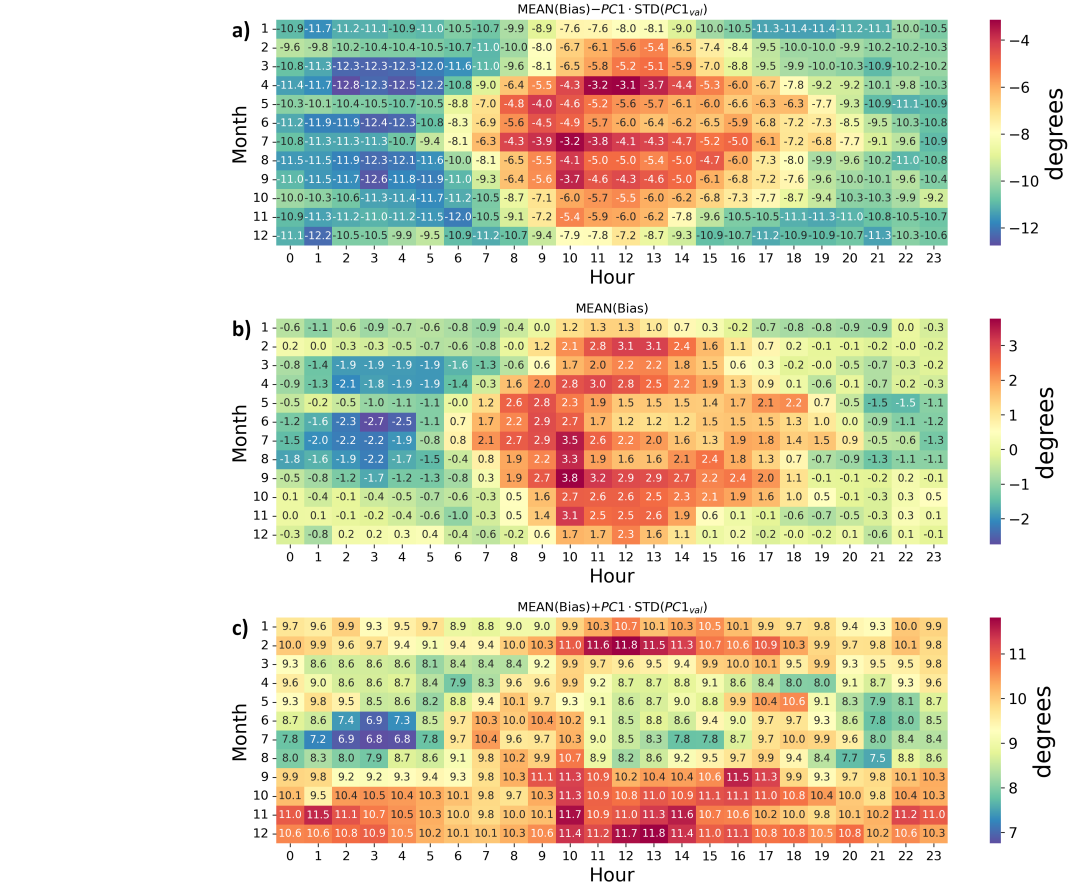

Figure 7. Wind direction biases (in degrees) in the ERA5 reanalysis dependent on month (y axis) and time of day (x axis). Spatially averaged bias is shown in (b). (c) shows spatially averaged bias plus 1 standard deviation of values of the PC1 between observation locations. (a) shows spatially averaged bias minus 1 standard deviation of values of the PC1 between observation locations.

respectively. When elevation difference is considered, EMD-EUR+ and NEWA show the strongest increases in the correlation versus the case when only real-world elevation is considered. For PC1 of the wind speed bias, the correlation with real-world elevation is only −0.16 for EMD-EUR+ and −0.15 for NEWA. However, when the elevation difference is considered, the correlation increases to 0.37 and 0.46 respectively. The correlations between real-world and model elevation are 0.93–0.94 for global reanalyses and 0.98–0.99 for mesoscale model datasets.

All correlations between the principal components of model biases and weighted elevation differences between model and real-world are statistically significant at the significance level of 0.05. The smallest number of masts was used when validating the NORA3 dataset, only 254. For 254 data points, the correlation coefficient with an absolute value greater than 0.12 is statistically significant at the significance level of 0.05. For other datasets, the correlation threshold is even lower. When the model elevation or the real-world elevation is considered individually, the correlation is not always statistically significant.

https://doi.org/10.5194/wes-2026-24
Preprint. Discussion started: 10 February 2026

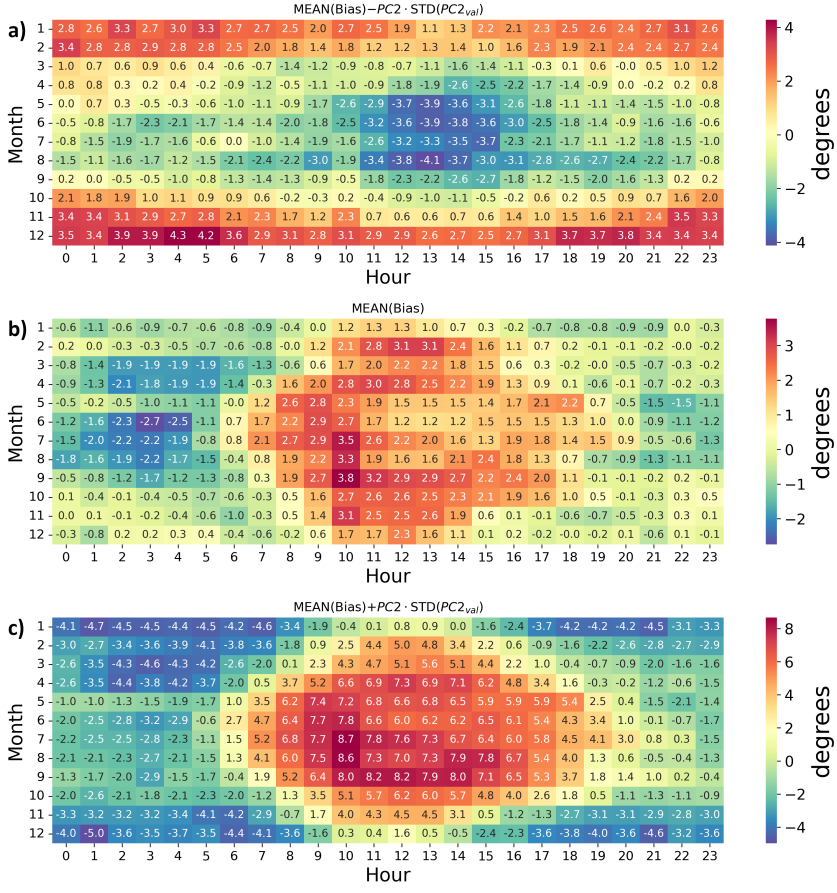

Figure 8. Wind direction biases (in degrees) in the ERA5 reanalysis dependent on month (y axis) and time of day (x axis). Spatially averaged bias is shown in (b). (c) shows spatially averaged bias plus 1 standard deviation of values of the PC2 between observation locations. (a) shows spatially averaged bias minus 1 standard deviation of values of the PC1 between observation locations.

While correlations between elevation difference and bias variables are statistically significant, in some cases they are weak and cannot be used to provide a hypothesis about a potential physical cause. However, it has to be kept in mind that the atmosphere is chaotic and model biases are caused by a lot of different physical phenomena. Therefore, if the fact of causation can be established, low correlation implies presence of noise in the data. In that case, correlation is used to measure the strength of the effect rather than to indicate the presence of the effect. For example, a correlation (R) of 0.3 between bias and elevation difference indicates that elevation difference explains 9 % of the variance (R^2) in model biases. In the discussion section, it is described which physical phenomena might theoretically cause wind biases in case when the model elevation differs from the real-world elevation.

Lets analyse how correlations of values of PCs of wind biases and elevation difference between model and real-world can be interpreted. The results show that, on average, if observations are performed above the model grid-cell elevation, then the

https://doi.org/10.5194/wes-2026-24
Preprint. Discussion started: 10 February 2026

Figure 9. Correlations between values of principal components that describe model biases and terrain variables (x axis) for different model datasets (y axis). WS denotes wind speed and WD denotes wind direction biases.

model underestimates the wind speed. The underestimation is stronger in winter than in summer and stronger during the night than during the day. Additionally, the model shows overall anti-clockwise wind direction bias. The bias is more anti-clockwise in winter than in summer and more anti-clockwise during the night than during the day. On the other hand, if observations are performed below the model grid-cell elevation then on average the model overestimates the wind speed. The overestimation is stronger in winter than in summer and stronger during the night than during the day. Additionally, the model shows overall clockwise wind direction bias. The bias is more clockwise in winter than in summer and more clockwise during the night than during the day.

3.1.1 100 m wind speed bias in ERA5

One of the objectives of the work was to assess how 100 m wind speed bias from ERA5 is inherited in downscaled mesoscale models. In Figure 6 it is clearly visible that there is a sharp decrease in the wind speed bias from 9:00 UTC to 10:00 UTC in the ERA5 reanalysis. The decrease is also visible in the data from the CERRA reanalysis. However, it is less prominent. Meanwhile, there is no noticeable unrealistic change in the wind speed bias between 9:00 and 10:00 UTC in the plots for NORA3, NEWA, and EMD-EUR+.

The prominence of 100 m wind speed bias in mesoscale model output can be explained by model initialisation strategies. CERRA reanalysis assimilates observations every three hours, and in this work data with a spin-up time of only one hour are used. Moreover, both CERRA and ERA5 are developed by the same organisation ECMWF. Therefore, the CERRA reanalysis is likely to be closer to the host reanalysis ERA5 than other downscaled products.

The NORA3 dataset uses a longer spin-up time of 3 hours than CERRA, which is likely to reduce the effect of bias. NEWA and EMD-EUR+ reinitialise model once a week. Moreover, they are always initialised at 0:00 UTC, during the 21:00–9:00 UTC assimilation window, which does not experience 100 m wind speed issues in the ERA5. Therefore, these models are less affected by the issue. However, it has to be kept in mind that all mesoscale models use boundary conditions from ERA5, which

https://doi.org/10.5194/wes-2026-24
Preprint. Discussion started: 10 February 2026

eawe european academy of wind energy
Open Access WIND ENERGY SCIENCE DISCUSSIONS

are regularly updated. In addition, NEWA and EMD-EUR+ are nudged towards ERA5. Therefore, they are likely to experience a performance drop due to the 100 m wind speed issue with ERA5, despite the issue not being directly observable in the plots of this work.

3.2 WRF model comparison

The results of the model comparison with observations suggested that wind speed and direction biases are correlated with the elevation difference between the models and the real-world. Moreover, the magnitude of the bias depends on the time of day and year. To provide a more robust support for the hypothesis, two WRF simulations using different terrain input datasets were performed and the modelled winds were compared. It was hypothesised that these models would show differences that are similar in nature to the differences between models and observations. When comparing two models, PCA was applied in a similar way as it was applied when comparing models and observations. However, instead of using only 508 observation locations, model differences were compared in all 250×520 grid-cells.

The loadings for the PCA of the model comparison are shown in Figure 10. The loadings of PC1 of the wind speed difference when comparing two models show similar diurnal and seasonal patterns as the loadings of PC1 of the wind speed when comparing models with observations (Figure 5). In case for wind direction difference, there is a difference from the case when comparing models with observations. When comparing models with observations PC1 describes the overall magnitude of the wind direction bias and PC2 describes diurnal and seasonal patterns of the wind direction bias. In case of comparing two models, the loadings of PC1 of the wind direction difference show similarities to the case with the wind speed. PC1 of the wind direction difference between models describes both the overall magnitude and the temporal patterns of the wind direction difference. A potential explanation of such difference is that when comparing two models there is no overall wind direction bias caused by improper reference direction calibration or subgrid obstacles.

For both wind speed and wind direction differences, values of PC1 show similar spatial patterns (Figure 11). PC1 shows slightly negative values over the sea and in Southern Sweden, where the terrain is simple. In northern parts of Sweden, where the terrain is complex, PC1 shows a high contrast in values: strongly positive and strongly negative. The patterns of these values follow the terrain. Strongly positive values are present in valleys, while strongly negative values are present on top of hills.

PC1 of the wind speed difference explains 75 % of the variance in wind speed differences between both WRF models. PC1 of the wind direction difference explains 22 % of the variance in wind direction differences between both WRF model simulations.

Similarly to observations, the principal components of the differences between two models show correlations with the elevation difference between these two models. Values of PC1 of the wind speed difference between models shows a 0.35 correlation with the elevation in 30 s model and 0.42 correlation with the elevation in 5 min model. When the weighted difference between elevations is considered, the correlation increases to 0.69. Values of PC1 of the wind direction difference between models shows a 0.05 correlation with the elevation in 30 s model and 0.12 correlation with the elevation in 5 min

https://doi.org/10.5194/wes-2026-24
Preprint. Discussion started: 10 February 2026

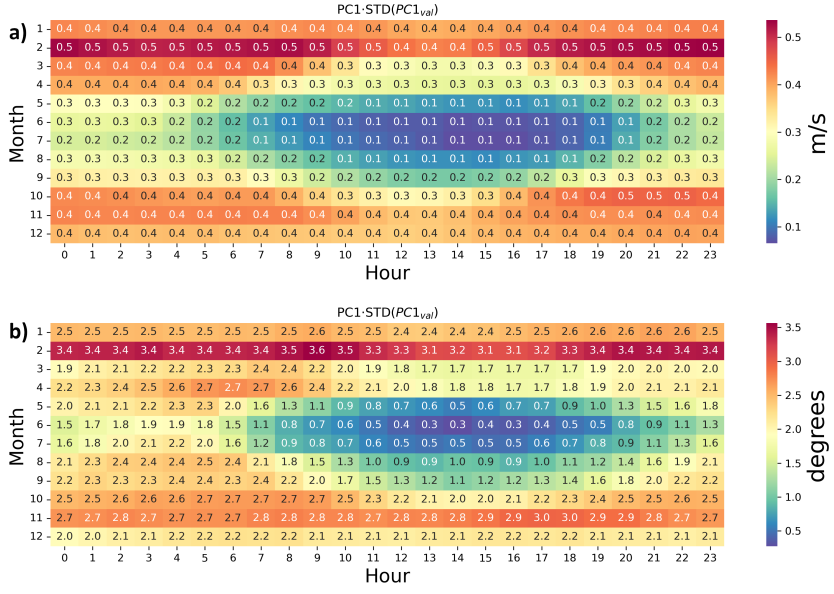

Figure 10. Model difference comparison. Loadings of the PC1 for wind speed difference (a) and wind direction difference (b) multiplied by the standard deviation of the PC1 values between all grid-points. Units are m s^{-1} for wind speed and degrees for wind direction.

model. When weighted difference between elevations is considered, the correlation increases to 0.56. The correlation between elevation in the 30 s model and the 5 min model is greater than 0.99.

Correlations between values of principal components of model differences and elevation differences can be interpreted similarly to the case when models and observations are compared. If the terrain elevation of a grid-cell in two models is the same, then models on average show small differences in wind speeds and wind directions. On the other hand, if the terrain elevation of a grid-cell differs between two models, the model in which the elevation is higher on average shows a higher wind speed and a more clockwise wind direction. The wind speed difference is higher in winter than in summer and higher during the night than during the day. The difference in wind direction is more clockwise in winter than in summer and more clockwise during the night than during the day.

By multiplying regression coefficients when explaining the bias with the elevation difference by the loadings of the principal components, it is possible to estimate the magnitude of the bias caused by the elevation difference. The elevation difference of 100 m between two models creates a difference in wind speed between 0.1 m s^{-1} in summer during the day and 0.9 m s^{-1} in winter. When comparing models with observations, the elevation difference showed an effect on the wind speed bias of approximately the same magnitude. The elevation difference of 100 m creates a difference in the wind direction between 0.4°in summer during the day and 5.6°in winter. However, the effects of the elevation difference on the wind direction bias cannot be clearly isolated from the observations since there is a large contribution to the wind direction bias from improper

https://doi.org/10.5194/wes-2026-24
Preprint. Discussion started: 10 February 2026

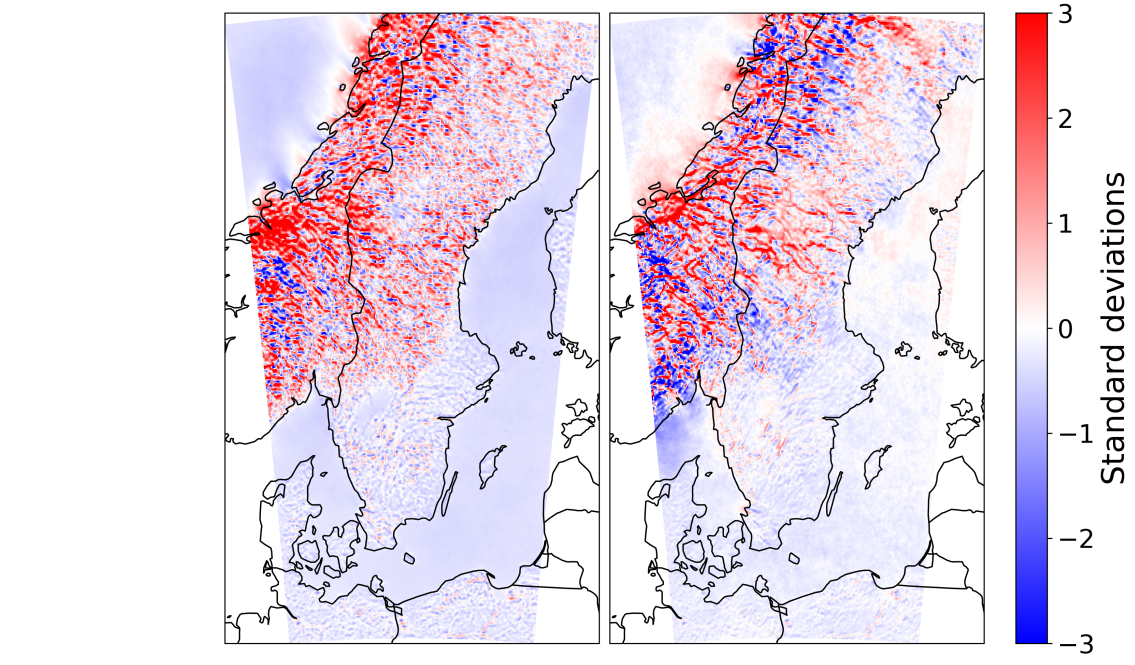

Figure 11. Values of PC1 for model differences of wind speed bias (left) and wind direction bias (right). Values are normalised by dividing a value of PC1 at each grid-point by the standard deviation of all PC1 values between all grid-points. Units are standard deviations above the average.

reference direction calibration or obstacles in the near proximity of the observation location. It is likely that the magnitude of the effect is similar as in the case when comparing two models.

While loadings of main principal components and correlations with terrain for model comparison and model-observation comparison look similar, spatial patterns of values of principal components on the first glance look different. When comparing models and observations, values of PC1 of the wind speed bias are more positive in simple terrain and more negative in complex terrain. On the other hand, when comparing two models, the values of PC1 of the wind speed difference are more negative on top of the hills, more positive inside valleys, and closer to zero in simple terrain. However, differences in spatial patterns of the values of principal components can be explained if we consider the fact that observation campaigns are usually performed on top of the hills. As observation campaigns are more likely to be performed on top of the hill, the strongly negative values of PC1 of the wind speed bias are more abundant than strongly positive values when comparing models to observations in the complex terrain. This explains more negative values of PC1 of wind speed bias in complex terrain in observations.

4 Discussion

Differences in model biases between parts of Europe have been observed before in the NEWA and ERA5 model datasets (Dörenkämper et al., 2020). They have shown that wind speed biases in Europe become more positive towards the north and

https://doi.org/10.5194/wes-2026-24
Preprint. Discussion started: 10 February 2026

more negative towards the east. Previous studies have identified that both the MERRA and MERRA2 reanalyses underestimate wind speeds in Northern and Southern Europe, while overestimating wind speeds in Central Europe (Staffell and Pfenninger, 2016; Monforti and Gonzalez-Aparicio, 2017). This work confirms the presence of the bias in MERRA2 and shows that the same bias is present in the ERA5 and JRA-3Q global reanalyses. Moreover, the bias is present in mesoscale datasets which perform dynamic downscaling. However, the magnitude of the bias is lower in mesoscale models. As spatial and temporal patterns of biases are consistent between global and mesoscale models, biases created by use of 10 m model winds, when interpolating winds at different heights, were much less significant than biases of models themselves.

More negative wind speed bias and lower modelled wind speed correlation in regions with complex orography have already been widely described in the literature before, e.g. Dörenkämper et al. (2020); Das and Baidya Roy (2024); Winstral et al. (2016); Hu et al. (2023); Laurila et al. (2021). This has led to conclusions that models generally underestimate wind speeds in complex terrains. However, the exact causes are still unclear. In this work, it was shown that considering the difference between real-world and model elevation significantly increases the correlation with bias. This leads to a possible physical explanation of the bias – model wind speed biases in complex terrain are caused by discrepancies between how terrain is represented in models and the real-world terrain. When observed winds are compared with the modelled winds, essentially winds over two different terrains are compared.

When comparing observation data with model data, it was observed that the wind speed bias is more negative in complex terrain regions. The results of the WRF modelling provided a better understanding of spatial patterns of wind biases. Wind speed bias is more negative (positive) if observations are performed above (below) the average model grid cell height. A similar pattern is true for the wind direction. If observation mast is located at a higher elevation than the model grid cell, the model is more likely to show more anti-clockwise wind direction bias, since in the Northern Hemisphere the wind direction is more anti-clockwise higher above the surface. Observation campaigns are usually performed at the potential locations of future wind farms. Therefore, they are likely to be performed on top of hills rather than inside the valleys. When the terrain is aggregated and smoothed, the elevation of the valley generally increases and the elevation of the hill generally decreases. Therefore, the elevation of the observation campaigns is usually higher than the elevation of the corresponding model grid cells.

The results of this work show that wind speed and direction biases in models are correlated with the elevation difference between the model and the real-world. The results of the comparison between models that use two different terrain datasets show that these biases can potentially be fixed by changing how the terrain is represented in the model. However, the results of this work do not directly provide any information on the exact underlying physical processes that cause biases. It is likely that multiple physical processes are affected by differences in the representation of the terrain between models and the real-world. These processes are discussed in further paragraphs.

Since the terrain in the models is smoothed out, heights of the hills and depths of the valleys are generally underestimated in the models. If the height of the hill is underestimated in the model, the model underestimates orographic speed-up, which causes it to underestimate wind speeds. Errors in estimating orographic speed-up have been described as a potential cause of wind speed bias before (Jiménez and Dudhia, 2012).

https://doi.org/10.5194/wes-2026-24
Preprint. Discussion started: 10 February 2026

Wind speed generally increases with height, and wind direction becomes more clockwise (in the Northern Hemisphere). If the height of the hill is underestimated in model, it is exposed to slower winds and more anti-clockwise wind direction. The relationship between topographic exposure and model wind speed biases has previously been observed by Pauscher et al. (2025). Topographic exposure is defined as the angle between the horizontal and the horizon when looking in a particular direction. It describes how exposed to or sheltered from winds the location is. A positive exposure angle indicates that the location is sheltered by the terrain, while a negative exposure angle indicates that it is exposed to winds.

Differences in topographic exposure can explain why the wind speed and direction biases are lower during the day than during the night. Assume that above the planetary boundary layer (PBL) wind flow is purely geostrophic with some wind speed and direction. Due to the friction force, near-surface winds are slower and more anti-clockwise (in the Northern Hemisphere). Within the PBL both wind speed and direction change continuously between these two values. If the atmosphere is more stable, less vertical mixing occurs, and the wind speed and direction change more uniformly throughout the boundary layer. On the other hand, if the atmosphere is unstable and the mixing is strong, strong vertical wind gradients occur near the very surface, and the change is slower at higher levels. Assume that an observation mast that measures wind speed at 100 m height above the ground level is located on top of a hill, that is 50 m above the model grid cell level. In the model the mast is exposed to winds at 100 m height, while in the real-world it is exposed to winds at 150 m height. During stable atmospheric conditions, the wind speed and direction differences between 100 m and 150 m heights are greater than during unstable conditions. Therefore, the difference between model output and observations is likely to be higher during stable conditions. Differences in topographic exposure can also explain the relationship between wind speed and wind direction biases.

Another possible cause of wind biases related to the terrain representation is differences between terrain slopes in the model and the real-world. Spatial aggregation of the terrain generally smooths out the slopes. Differences in terrain slopes affect solar radiation received by the surface, which affects vertical momentum transfer due to convection. If we assume that the winds at higher levels of the atmosphere are modelled correctly, in the Northern Hemisphere models overestimating (underestimating) vertical transport of momentum can cause clockwise (anticlockwise) near-surface wind direction bias and positive (negative) wind speed bias (Sandu et al., 2020).

The elevation difference between models and the real-world statistically explains wind biases locally, i.e. within the same grid-cell. However, it has to be kept in mind that the winds in the atmosphere are in constant motion. Therefore, wind biases can propagate spatially, i.e. if the model underestimates winds at a certain location, it is more likely to underestimate winds at downwind locations. The analysis of this work focused only on identifying biases caused by local terrain effects. However, it is reasonable to assume fixing biases locally would also improve non-local biases.

In observations, for wind speed, PC1 describes both differences in magnitude and diurnal cycle of bias between different parts of Europe. On the other hand, for the wind direction, PC1 describes differences in overall magnitude of the bias, while PC2 describes differences in the diurnal cycle. As values of PC1 of the wind direction bias shows no clear spatial patterns, it is potentially caused either by the obstacles in close proximity of the observation mast or by the improperly calibrated reference wind direction. As wind speed and direction biases are potentially related, it is possible that due to elevation differences between model and real-world, modelled wind direction can have an overall clockwise or anti-clockwise bias. However, since

https://doi.org/10.5194/wes-2026-24
Preprint. Discussion started: 10 February 2026

there is a strong overall wind direction bias that is potentially caused by an improper reference direction calibration, the bias shows only a weak signal in the observation data. Meanwhile, when comparing two WRF model runs using different terrains, the overall wind direction bias that is correlated with the elevation difference can be seen much more clearly.

Jiménez and Dudhia (2012) has previously noted that the WRF model overestimates wind speeds in valleys and underestimates wind speeds on top of hills. The study suggested and implemented wind correction using the Laplace of the elevation, which quantifies the difference in elevation between the corresponding and four adjacent grid cells. The Laplace of the elevation was considered as the explanatory variable for model biases during the exploratory data analysis of this work. However, Laplace of the elevation showed weaker explanatory power than the elevation difference. When comparing principal components of the model difference, weighted differences in the Laplace of elevation showed correlations of 0.43 and 0.43 for values of PC1 of wind speed and wind direction, respectively. Compared to 0.69 and 0.56 for the case when weighted elevation difference is considered.

Jiménez and Dudhia (2012, 2013) have noted that the model performance in modelling winds in complex terrain can be significantly improved by choosing a more representative model grid point both horizontally and vertically. These studies have used a subjective approach, which cannot be generalised when assessing wind resources in larger areas. Choosing the appropriate model grid-point for representing the observation location should be physically justified. The results of this work suggest that choosing a nearby model grid-point that better matches the observation elevation has the potential to improve the wind speed bias. However, it cannot be guaranteed that there exists a model grid-point that matches the observation elevation. These studies also suggested choosing the appropriate grid-point not only horizontally, but also vertically. However, for wind energy applications, knowledge of the entire wind profile within the lowest few hundred metres is necessary, which would make the procedure of choice more complicated.

Microscale modelling has the potential to improve modelled winds in complex terrain. However, due to computational limitations, performing complete computational fluid dynamics (CFD) simulations is possible only for individual sites. For wind resource assessment on a larger scale, the WAsP linear model has been applied by Dörenkämper et al. (2020). However, the study has reported that the linear model largely overestimates winds in the most complex orography, since the assumptions of the linear model do not hold. While microscale modelling can improve the bias caused by terrain representation, it has to be kept in mind that microscale models usually cover small domains and use boundary conditions from mesoscale models. Therefore, improving biases related to terrain representation in mesoscale models is important for wind resource assessment both on the mesoscale and the microscale.

5 Conclusions

In this work, a large dataset of tall-mast and remote sensing device wind observations was used to address systematic issues of multiple atmospheric model datasets. To the authors' knowledge, such large scale comparisons between modelled and observed winds at wind turbine rotor heights have not been conducted before. It was shown that all seven different atmospheric models share the same bias when modelling wind speeds at wind turbine rotor heights. Models generally underestimate wind speeds

https://doi.org/10.5194/wes-2026-24
Preprint. Discussion started: 10 February 2026

in mountainous regions — Scandinavian mountains and Southern Europe, while overestimating them in the Central European Plain. Moreover, it was shown that the diurnal and seasonal cycles of wind speed biases also differ between these parts of Europe. It was observed that wind direction biases share the same diurnal and spatial patterns as wind speed biases.

Both wind speed and direction bias showed a meaningful correlation with the elevation difference between the model and the real-world. These correlations provided a potential physical explanation for these biases. Differences between modelled and observed winds can be caused by the incomplete representation of real-world terrain in the model grid. Specifically, model biases can be explained by considering that the height above the mean sea level at which the model outputs winds does not directly represent the height at which observations are performed. These differences in height influence how several physical processes are represented in the model, which impact modelled winds. The results of this work cannot distinguish the contribution of different physical processes to this wind bias. However, the results suggest that the bias can possibly be improved by modifying the model terrain so that it matches the real-world terrain elevation more closely.

WRF numerical modelling was carried out to provide more robust support for the hypothesis about the cause of differences between modelled and observed winds. Modelled winds of two one-year runs using different input terrain datasets, but otherwise the same setups were compared. The differences in winds between two different models showed similar spatial and temporal patterns as differences between models and observations. Similarly, to observations, the principal components that describe these patterns showed a high correlation with the differences in elevation between the datasets. However, results of modelling provided a better understanding about biases in complex terrain. WRF modelling showed that the negative wind speed bias is present on top of the hills and positive bias is present in valleys. Meanwhile, when compared to observations, models generally underestimate wind speeds in complex terrain, since observation campaigns are more likely to be conducted on top of the hills.

Data availability. Observation data from the EMD internal mast database and EMD-EUR+ dataset are not publicly available. Data from NORA3 model dataset is available from https://thredds.met.no/thredds/projects/nora3.html. Data from CERRA reanalysis is available from https://cds.climate.copernicus.eu/datasets/reanalysis-cerra-height-levels. Data from ERA5 reanalysis is available from https://cds.climate.copernicus.eu/datasets/reanalysis-era5-single-levels. Data from MERRA2 reanalysis is available from https://disc.gsfc.nasa.gov/datasets?project=MERRA-2. Data from NEWA model dataset is available from https://map.neweuropeanwindatlas.eu/. Data from JRA-3Q reanalysis is available from https://gdex.ucar.edu/datasets/d640001/.

https://doi.org/10.5194/wes-2026-24
Preprint. Discussion started: 10 February 2026

eawe european academy of wind energy
Open Access WIND ENERGY SCIENCE DISCUSSIONS

Appendix A: WRF setup

Table A1. Setup of the WRF models used in this work.

WRF version	4.5.1.
Domain	Single 810×1620 km domain centred on Sweden.
Grid	3 km grid spacing. 270×540 grid cells. 10 cell wide buffer zone at the boundary.
Vertical levels	50
Simulation length	Simulation covering the entire 2011 stitching together 48 h runs with 6 h spin-up.
Terrain data	GMTED2010 with 30 s and 5 min resolution
Dynamical forcing	Hourly ERA5 data on surface and pressure levels
Time step	12 s
PBL scheme	MYJ
Surface layer scheme	Eta Similarity
Land surface model	Noah
Cloud microphysics scheme	Ferrier Eta
Radiation scheme	RRTMG
Cumulus scheme	None

Appendix B: Results of PCA for all model datasets

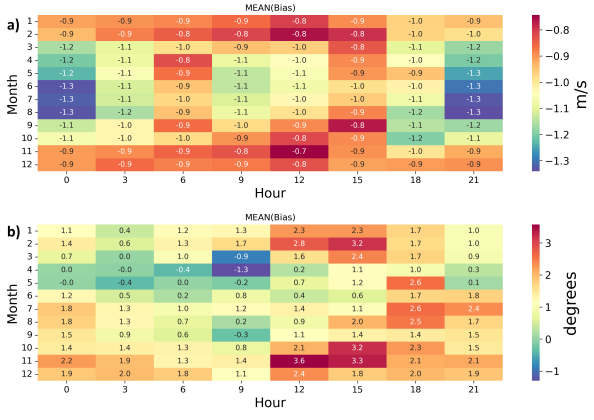

Figure B1. Spatially averaged wind speed biases (in $\mathrm{m\,s^{-1}}$) (a) and wind direction biases (in degrees) (b) in JRA-3Q reanalysis dependent on month (y axis) and time of day (x axis).

https://doi.org/10.5194/wes-2026-24
Preprint. Discussion started: 10 February 2026

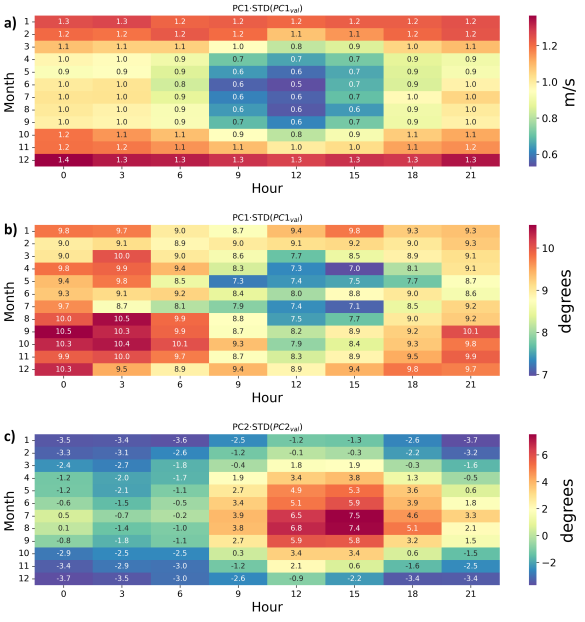

Figure B2. JRA-3Q reanalysis and observation comparison. Loadings of the PC1 for wind speed bias (a), PC1 of wind direction bias (b) and PC2 of wind direction bias (c). Multiplied by the standard deviation of values of the corresponding PC.

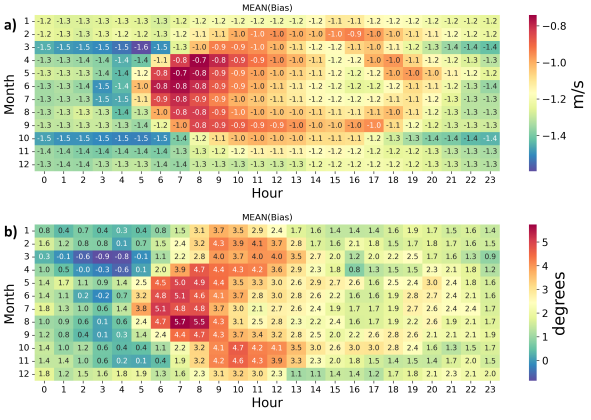

Figure B3. Spatially averaged wind speed biases (in m s^{-1}) (a) and wind direction biases (in degrees) (b) in MERRA2 reanalysis dependent on month (y axis) and time of day (x axis).

https://doi.org/10.5194/wes-2026-24
Preprint. Discussion started: 10 February 2026

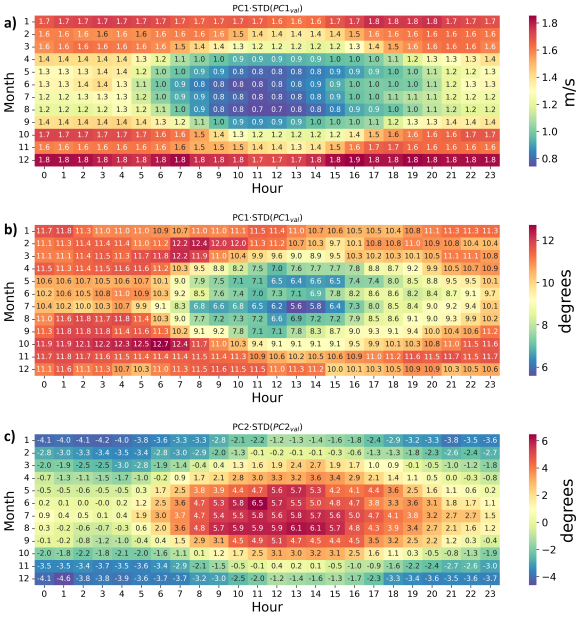

Figure B4. MERRA2 reanalysis and observation comparison. Loadings of the PC1 for wind speed bias (a), PC1 of wind direction bias (b) and PC2 of wind direction bias (c). Multiplied by the standard deviation of values of the corresponding PC.

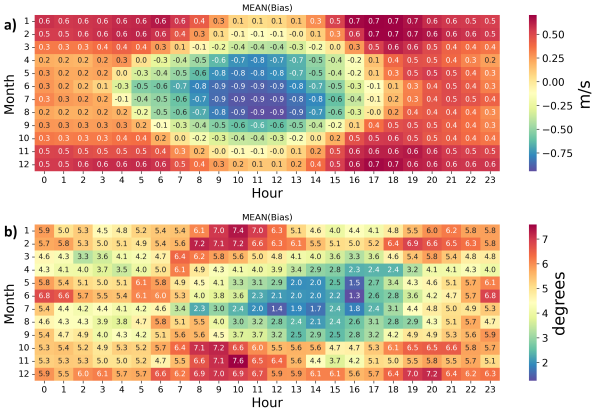

Figure B5. Spatially averaged wind speed biases (in m s^{-1}) (a) and wind direction biases (in degrees) (b) in NEWA model dataset dependent on month (y axis) and time of day (x axis).

https://doi.org/10.5194/wes-2026-24
Preprint. Discussion started: 10 February 2026

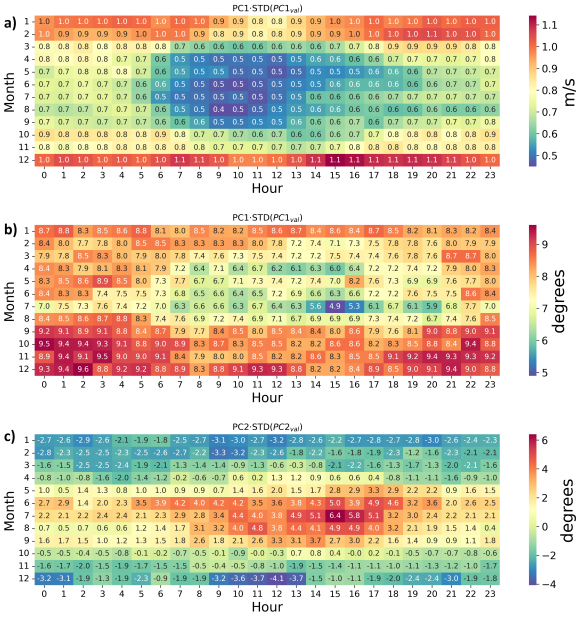

Figure B6. NEWA model dataset and observation comparison. Loadings of the PC1 for wind speed bias (a), PC1 of wind direction bias (b) and PC2 of wind direction bias (c). Multiplied by the standard deviation of values of the corresponding PC.

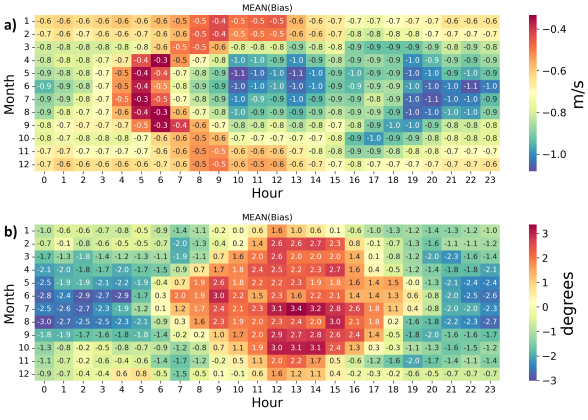

Figure B7. Spatially averaged wind speed biases (in m s^{-1}) (a) and wind direction biases (in degrees) (b) in CERRA model dataset dependent on month (y axis) and time of day (x axis).

https://doi.org/10.5194/wes-2026-24
Preprint. Discussion started: 10 February 2026

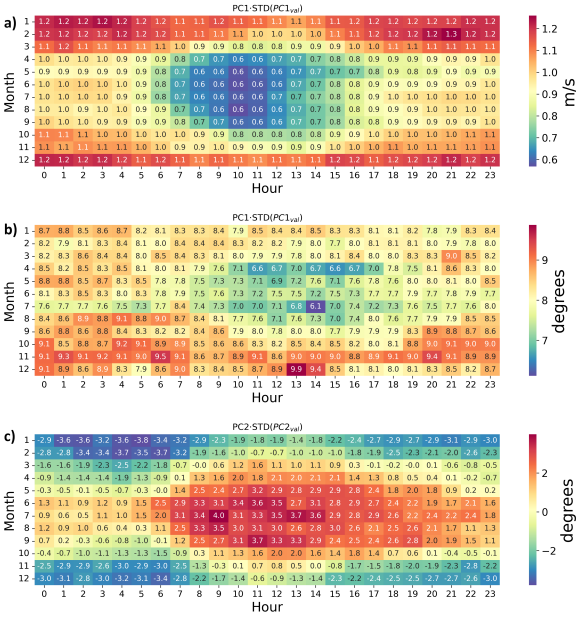

Figure B8. CERRA model dataset and observation comparison. Loadings of the PC1 for wind speed bias (a), PC1 of wind direction bias (b) and PC2 of wind direction bias (c). Multiplied by the standard deviation of values of the corresponding PC.

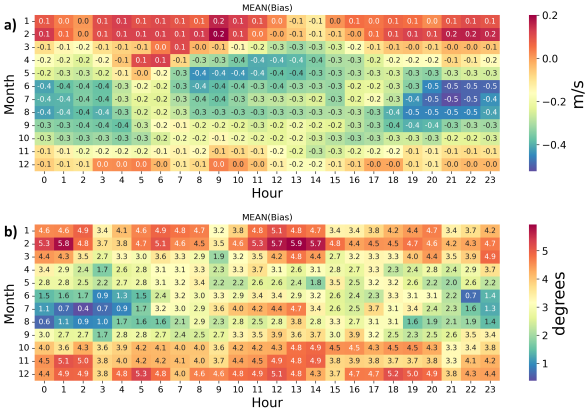

Figure B9. Spatially averaged wind speed biases (in m s^{-1}) (a) and wind direction biases (in degrees) (b) in NORA3 model dataset dependent on month (y axis) and time of day (x axis).

https://doi.org/10.5194/wes-2026-24
Preprint. Discussion started: 10 February 2026

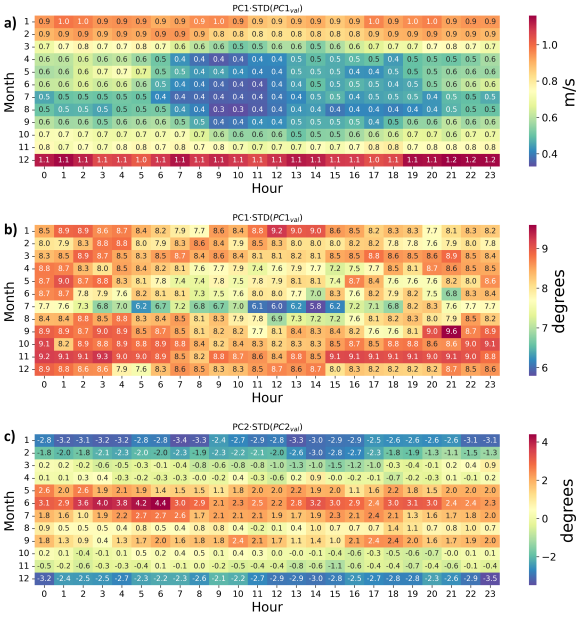

Figure B10. NORA3 model dataset and observation comparison. Loadings of the PC1 for wind speed bias (a), PC1 of wind direction bias (b) and PC2 of wind direction bias (c). Multiplied by the standard deviation of values of the corresponding PC.

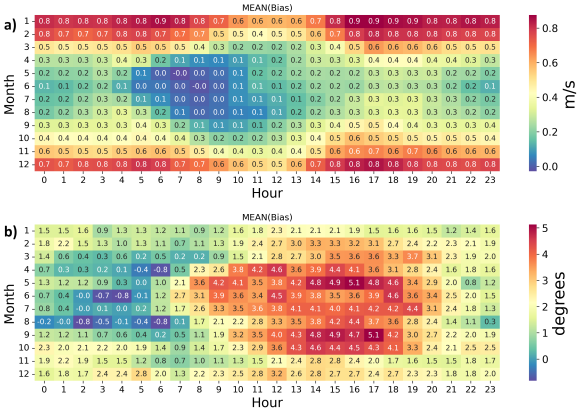

Figure B11. Spatially averaged wind speed biases (in $\mathrm{m\,s^{-1}}$) (a) and wind direction biases (in degrees) (b) in EMD-EUR+ model dataset dependent on month (y axis) and time of day (x axis).

https://doi.org/10.5194/wes-2026-24
Preprint. Discussion started: 10 February 2026

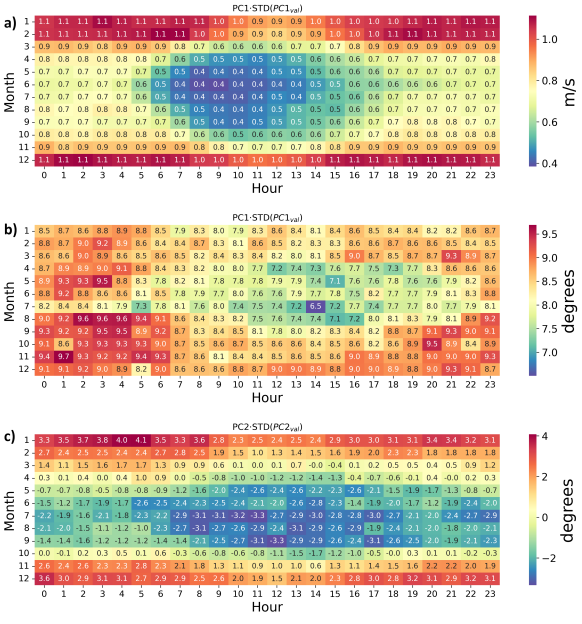

Figure B12. EMD-EUR+ model dataset and observation comparison. Loadings of the PC1 for wind speed bias (a), PC1 of wind direction bias (b) and PC2 of wind direction bias (c). Multiplied by the standard deviation of values of the corresponding PC.

https://doi.org/10.5194/wes-2026-24
Preprint. Discussion started: 10 February 2026

eawe european academy of wind energy
Open Access WIND ENERGY SCIENCE DISCUSSIONS

Author contributions. MP designed the study, performed model validation against measurements, performed WRF simulations, analysed the results, prepared the figures. TS, LS and AH provided scientific supervision. MP wrote the draft for the manuscript. All authors contributed to the final version of the manuscript.

Competing interests. MP and LS work at the EMD International A/S, which commercially provides data from the EMD-EUR+ model dataset and EMD's internal mast database. AH is a member of the editorial board of Wind Energy Science.

Acknowledgements. Maksims Pogumirskis has received funding from the European Union's Horizon Europe research and innovation programme (HORIZON-MSCA-2022-DN-01-01) under the Marie Sklodowska-Curie grant agreement no. 101119550 (AptWind).

https://doi.org/10.5194/wes-2026-24
Preprint. Discussion started: 10 February 2026

eawe european academy of wind energy
Open Access WIND ENERGY SCIENCE DISCUSSIONS

References

Belmonte Rivas, M. and Stoffelen, A.: Characterizing ERA-Interim and ERA5 surface wind biases using ASCAT, Ocean Science, 15, 831–852, https://doi.org/10.5194/os-15-831-2019, 2019.

Bethere, L., Sennikovs, J., and Bethers, U.: Climate indices for the Baltic states from principal component analysis, Earth System Dynamics, 8, 951–962, https://doi.org/10.5194/esd-8-951-2017, 2017.

Carvalho, D.: An Assessment of NASA's GMAO MERRA-2 Reanalysis Surface Winds, Journal of Climate, 32, 8261–8281, https://doi.org/10.1175/JCLI-D-19-0199.1, 2019.

Cheynet, E., Solbrekke, I. M., Diezel, J. M., and Reuder, J.: A one-year comparison of new wind atlases over the North Sea, Journal of Physics: Conference Series, 2362, 012 009, https://doi.org/10.1088/1742-6596/2362/1/012009, 2022.

Das, A. and Baidya Roy, S.: JRA55 is the best reanalysis representing observed near-surface wind speeds over India, Atmospheric Research, 297, 107 111, https://doi.org/https://doi.org/10.1016/j.atmosres.2023.107111, 2024.

Dörenkämper, M., Olsen, B. T., Witha, B., Hahmann, A. N., Davis, N. N., Barcons, J., Ezber, Y., García-Bustamante, E., González-Rouco, J. F., Navarro, J., Sastre-Marugán, M., Sīle, T., Trei, W., Žagar, M., Badger, J., Gottschall, J., Sanz Rodrigo, J., and Mann, J.: The Making of the New European Wind Atlas – Part 2: Production and evaluation, Geoscientific Model Development, 13, 5079–5102, https://doi.org/10.5194/gmd-13-5079-2020, 2020.

European Commission: Commission sets out immediate actions to support the European wind power industry, https://ec.europa.eu/commission/presscorner/detail/en/ip_23_5185, accessed: 2025-03-24, 2023.

Gelaro, R., McCarty, W., Suárez, M. J., Todling, R., Molod, A., Takacs, L., Randles, C. A., Darmenov, A., Bosilovich, M. G., Reichle, R., Wargan, K., Coy, L., Cullather, R., Draper, C., Akella, S., Buchard, V., Conaty, A., da Silva, A. M., Gu, W., Kim, G.-K., Koster, R., Lucchesi, R., Merkova, D., Nielsen, J. E., Partyka, G., Pawson, S., Putman, W., Rienecker, M., Schubert, S. D., Sienkiewicz, M., and Zhao, B.: "The Modern-Era Retrospective Analysis for Research and Applications, Version 2 (MERRA-2)", Journal of Climate, 30, 5419 – 5454, https://doi.org/10.1175/JCLI-D-16-0758.1, 2017.

Gualtieri, G.: Reliability of ERA5 Reanalysis Data for Wind Resource Assessment: A Comparison against Tall Towers, Energies, 14, https://doi.org/10.3390/en14144169, 2021.

Haakenstad, H., Øyvind Breivik, Furevik, B. R., Reistad, M., Bohlinger, P., and Aarnes, O. J.: NORA3: A Nonhydrostatic High-Resolution Hindcast of the North Sea, the Norwegian Sea, and the Barents Sea, Journal of Applied Meteorology and Climatology, 60, 1443 – 1464, https://doi.org/10.1175/JAMC-D-21-0029.1, 2021.

Hahmann, A. N., Sīle, T., Witha, B., Davis, N. N., Dörenkämper, M., Ezber, Y., García-Bustamante, E., González-Rouco, J. F., Navarro, J., Olsen, B. T., and Söderberg, S.: The making of the New European Wind Atlas – Part 1: Model sensitivity, Geoscientific Model Development, 13, 5053–5078, https://doi.org/10.5194/gmd-13-5053-2020, 2020.

Hersbach, H., Bell, B., Berrisford, P., Hirahara, S., Horányi, A., Muñoz-Sabater, J., Nicolas, J., Peubey, C., Radu, R., Schepers, D., Simmons, A., Soci, C., Abdalla, S., Abellan, X., Balsamo, G., Bechtold, P., Biavati, G., Bidlot, J., Bonavita, M., De Chiara, G., Dahlgren, P., Dee, D., Diamantakis, M., Dragani, R., Flemming, J., Forbes, R., Fuentes, M., Geer, A., Haimberger, L., Healy, S., Hogan, R. J., Hólm, E., Janisková, M., Keeley, S., Laloyaux, P., Lopez, P., Lupu, C., Radnoti, G., de Rosnay, P., Rozum, I., Vamborg, F., Villaume, S., and Thépaut, J.-N.: The ERA5 global reanalysis, Quarterly Journal of the Royal Meteorological Society, 146, 1999–2049, https://doi.org/https://doi.org/10.1002/qj.3803, 2020.

https://doi.org/10.5194/wes-2026-24
Preprint. Discussion started: 10 February 2026

Hollingsworth, A.: Validation and diagnosis of atmospheric models, Dynamics of Atmospheres and Oceans, 20, 227–246, https://doi.org/https://doi.org/10.1016/0377-0265(94)90019-1, forecasting weather and climate since, 1994.

Hu, W., Scholz, Y., Yeligeti, M., Bremen, L., and Deng, Y.: Downscaling ERA5 wind speed data: a machine learning approach considering topographic influences, Environmental Research Letters, 18, https://doi.org/10.1088/1748-9326/aceb0a, 2023.

Jiménez, P. A. and Dudhia, J.: Improving the Representation of Resolved and Unresolved Topographic Effects on Surface Wind in the WRF Model, Journal of Applied Meteorology and Climatology, 51, 300 – 316, https://doi.org/10.1175/JAMC-D-11-084.1, 2012.

Jiménez, P. A. and Dudhia, J.: On the Ability of the WRF Model to Reproduce the Surface Wind Direction over Complex Terrain, Journal of Applied Meteorology and Climatology, 52, 1610 – 1617, https://doi.org/10.1175/JAMC-D-12-0266.1, 2013.

Jolliffe, I. T.: Principal Component Analysis, Springer Series in Statistics, Springer New York, NY, 2 edn., ISBN 978-0-387-95442-4, https://doi.org/10.1007/b98835, springer Science+Business Media, Published: 01 October 2002, 2002.

Jourdier, B.: Evaluation of ERA5, MERRA-2, COSMO-REA6, NEWA and AROME to simulate wind power production over France, Advances in Science and Research, 17, 63–77, https://doi.org/10.5194/asr-17-63-2020, 2020.

Jourdier, B., Diaz, C., and Dubus, L.: Evaluation of CERRA for wind energy applications, in: EMS Annual Meeting 2023, Bratislava, Slovakia, https://doi.org/10.5194/ems2023-311, 2023.

Kalverla, P. C., Holtslag, A. A. M., Ronda, R. J., and Steeneveld, G.-J.: Quality of wind characteristics in recent wind atlases over the North Sea, Quarterly Journal of the Royal Meteorological Society, 146, 1498–1515, https://doi.org/https://doi.org/10.1002/qj.3748, 2020.

Kosaka, Y., Kobayashi, S., Harada, Y., Kobayashi, C., Naoe, H., Yoshimoto, K., Harada, M., Goto, N., Chiba, J., Miyaoka, K., Sekiguchi, R., Deushi, M., Kamahori, H., Nakaegawa, T., Tanaka, T. Y., Tokuhiro, T., Sato, Y., Matsushita, Y., and Onogi, K.: The JRA-3Q Reanalysis, Journal of the Meteorological Society of Japan. Ser. II, 102, 49–109, https://doi.org/10.2151/jmsj.2024-004, 2024.

Kuru, S.: Evaluating the accuracy of NEWA, ERA5 and NORA3 in predicting onshore wind conditions: a comparative study using ICOS meteorological mast data in Sweden, Master of science dissertation, Uppsala University, Department of Earth Sciences, Campus Gotland, Uppsala, Sweden, 2023.

Laurila, T. K., Sinclair, V. A., and Gregow, H.: Climatology, variability, and trends in near-surface wind speeds over the North Atlantic and Europe during 1979–2018 based on ERA5, International Journal of Climatology, 41, 2253–2278, https://doi.org/https://doi.org/10.1002/joc.6957, 2021.

Meyer, P. J. and Gottschall, J.: How do NEWA and ERA5 compare for assessing offshore wind resources and wind farm siting conditions?, Journal of Physics: Conference Series, 2151, 012 009, https://doi.org/10.1088/1742-6596/2151/1/012009, 2022.

Mi, X. and Liu, P.: A Comparative Study of Near-Surface Wind Speed Observations and Reanalysis Datasets in China Over the Past 38 Years, International Journal of Climatology, https://doi.org/https://doi.org/10.1002/joc.8738, 2024.

Miao, H., Dong, D., Huang, G., Hu, K., Tian, Q., and Gong, Y.: Evaluation of Northern Hemisphere surface wind speed and wind power density in multiple reanalysis datasets, Energy, 200, 117 382, https://doi.org/https://doi.org/10.1016/j.energy.2020.117382, 2020.

Monforti, F. and Gonzalez-Aparicio, I.: Comparing the impact of uncertainties on technical and meteorological parameters in wind power time series modelling in the European Union, Applied Energy, 206, 439–450, https://doi.org/https://doi.org/10.1016/j.apenergy.2017.08.217, 2017.

Owens, R. G. and Hewson, T. D.: ECMWF Forecast User Guide, ECMWF, https://doi.org/10.21957/m1cs7h, 2018.

Pauscher, L., Geiger, D., Wirth, M., Yuan, D., Weber, H., and Callies, D.: Downscaling reanalysis models using a simple data-driven approach based on topography and atmospheric conditions, in: Proceedings of the Wind Energy Science Conference (WESC 2025), Wind Energy Science Conference, Nantes, France, 24–27 June 2025, 2025.

https://doi.org/10.5194/wes-2026-24
Preprint. Discussion started: 10 February 2026

Pogumirskis, M., Sīle, T., Seņņikovs, J., and Bethers, U.: PCA analysis of wind direction climate in the baltic states, Tellus A: Dynamic Meteorology and Oceanography, 73, 1–16, https://doi.org/10.1080/16000870.2021.1962490, 2021.

Ramon, J., Lledó, L., Torralba, V., Soret, A., and Doblas-Reyes, F. J.: What global reanalysis best represents near-surface winds?, Quarterly Journal of the Royal Meteorological Society, 145, 3236–3251, https://doi.org/https://doi.org/10.1002/qj.3616, 2019.

Ridal, M., Bazile, E., Le Moigne, P., Randriamampianina, R., Schimanke, S., Andrae, U., Berggren, L., Brousseau, P., Dahlgren, P., Edvinsson, L., El-Said, A., Glinton, M., Hagelin, S., Hopsch, S., Isaksson, L., Medeiros, P., Olsson, E., Unden, P., and Wang, Z. Q.: CERRA, the Copernicus European Regional Reanalysis system, Quarterly Journal of the Royal Meteorological Society, 150, 3385–3411, https://doi.org/https://doi.org/10.1002/qj.4764, 2024.

Rouholahnejad, F., Meyer, P. J., and Gottschall, J.: Collocating wind data: A case study on the verification of the CERRA dataset, Journal of Physics: Conference Series, 2875, 012 016, https://doi.org/10.1088/1742-6596/2875/1/012016, 2024.

Sandu, I., Zadra, A., and Wedi, N.: Impact of orographic drag on forecast skill, ECMWF Newsletter, 150, published January 2017, 2017.

Sandu, I., Bechtold, P., Nuijens, L., Beljaars, A., and Brown, A.: On the causes of systematic forecast biases in near-surface wind direction over the oceans, https://doi.org/10.21957/wggbl43u, 2020.

Solbrekke, I. M., Sorteberg, A., and Haakenstad, H.: The 3 km Norwegian reanalysis (NORA3) – a validation of offshore wind resources in the North Sea and the Norwegian Sea, Wind Energy Science, 6, 1501–1519, https://doi.org/10.5194/wes-6-1501-2021, 2021.

Spangehl, T., Borsche, M., Niermann, D., Kaspar, F., Schimanke, S., Brienen, S., Möller, T., and Brast, M.: Intercomparing the quality of recent reanalyses for offshore wind farm planning in Germany's exclusive economic zone of the North Sea, Advances in Science and Research, 20, 109–128, https://doi.org/10.5194/asr-20-109-2023, 2023.

Staffell, I. and Pfenninger, S.: Using bias-corrected reanalysis to simulate current and future wind power output, Energy, 114, 1224–1239, https://doi.org/https://doi.org/10.1016/j.energy.2016.08.068, 2016.

Svenningsen, L., Thøgersen, M., and Sørensen, T.: Validation of EMD-WRF EUROPE+ (ERA5) mesoscale dataset, Tech. rep., EMD International A/S, https://help.emd.dk/knowledgebase/content/TechNotes/TechnicalNote7_EMDWRF_EUROPE_Validation.pdf, 2020.

Torralba, V., Doblas-Reyes, F. J., and Gonzalez-Reviriego, N.: Uncertainty in recent near-surface wind speed trends: a global reanalysis intercomparison, Environmental Research Letters, 12, 114 019, https://doi.org/10.1088/1748-9326/aa8a58, 2017.

United Nations Climate Change (UNFCCC): The Paris Agreement, https://unfccc.int/process-and-meetings/the-paris-agreement, accessed: 2025-03-24.

Winstral, A., Jonas, T., and Helbig, N.: Statistical Downscaling of Gridded Wind Speed Data Using Local Topography, Journal of Hydrometeorology, 18, https://doi.org/10.1175/JHM-D-16-0054.1, 2016.

Zhi, M. H.: Accuracy of Energy Estimation for Small Wind Farms Based on Mesoscale Wind Data, Bachelor of science dissertation, Uppsala University, Department of Earth Sciences, Campus Gotland, 2023.